F/A-18 Performance Benefits Measured During the Autonomous Formation Flight Project

M. Jake Vachon, Ronald J. Ray, Kevin R. Walsh, and Kimberly Ennix
NASA Dryden Flight Research Center
Edwards, California

September 2003

The NASA STI Program Office…in Profile

Since its founding, NASA has been dedicated to the advancement of aeronautics and space science. The NASA Scientific and Technical Information (STI) Program Office plays a key part in helping NASA maintain this important role.

The NASA STI Program Office is operated by Langley Research Center, the lead center for NASA's scientific and technical information. The NASA STI Program Office provides access to the NASA STI Database, the largest collection of aeronautical and space science STI in the world. The Program Office is also NASA's institutional mechanism for disseminating the results of its research and development activities. These results are published by NASA in the NASA STI Report Series, which includes the following report types:

- TECHNICAL PUBLICATION. Reports of completed research or a major significant phase of research that present the results of NASA programs and include extensive data or theoretical analysis. Includes compilations of significant scientific and technical data and information deemed to be of continuing reference value. NASA's counterpart of peer-reviewed formal professional papers but has less stringent limitations on manuscript length and extent of graphic presentations.

- TECHNICAL MEMORANDUM. Scientific and technical findings that are preliminary or of specialized interest, e.g., quick release reports, working papers, and bibliographies that contain minimal annotation. Does not contain extensive analysis.

- CONTRACTOR REPORT. Scientific and technical findings by NASA-sponsored contractors and grantees.

- CONFERENCE PUBLICATION. Collected papers from scientific and technical conferences, symposia, seminars, or other meetings sponsored or cosponsored by NASA.

- SPECIAL PUBLICATION. Scientific, technical, or historical information from NASA programs, projects, and mission, often concerned with subjects having substantial public interest.

- TECHNICAL TRANSLATION. English-language translations of foreign scientific and technical material pertinent to NASA's mission.

Specialized services that complement the STI Program Office's diverse offerings include creating custom thesauri, building customized databases, organizing and publishing research results…even providing videos.

For more information about the NASA STI Program Office, see the following:

- Access the NASA STI Program Home Page at *http://www.sti.nasa.gov*

- E-mail your question via the Internet to help@sti.nasa.gov

- Fax your question to the NASA Access Help Desk at (301) 621-0134

- Telephone the NASA Access Help Desk at (301) 621-0390

- Write to:
  NASA Access Help Desk
  NASA Center for AeroSpace Information
  7121 Standard Drive
  Hanover, MD 21076-1320

NASA/TM-2003-210734

F/A-18 Performance Benefits Measured During the Autonomous Formation Flight Project

M. Jake Vachon, Ronald J. Ray, Kevin R. Walsh, and Kimberly Ennix
NASA Dryden Flight Research Center
Edwards, California

Available from the following:

ABSTRACT

The Autonomous Formation Flight (AFF) project at the NASA Dryden Flight Research Center (Edwards, California) investigated performance benefits resulting from formation flight, such as reduced aerodynamic drag and fuel consumption. To obtain data on performance benefits, a trailing F/A-18 airplane flew within the wingtip-shed vortex of a leading F/A-18 airplane. The pilot of the trail airplane used advanced station-keeping technology to aid in positioning the trail airplane at precise locations behind the lead airplane. The specially instrumented trail airplane was able to obtain accurate fuel flow measurements and to calculate engine thrust and vehicle drag. A maneuver technique developed for this test provided a direct comparison of performance values while flying in and out of the vortex. Based on performance within the vortex as a function of changes in vertical, lateral, and longitudinal positioning, these tests explored design-drivers for autonomous station-keeping control systems. Observations showed significant performance improvements over a large range of trail positions tested. Calculations revealed maximum drag reductions of over 20 percent, and demonstrated maximum reductions in fuel flow of just over 18 percent.

NOMENCLATURE

Acronyms

AFF   Autonomous Formation Flight (project)

AP   area pressure thrust calculation technique

ATC   automatic throttle control

BL   baseline maneuver

DPS   digital performance simulation (computer model)

FF   formation flight, within influence of the vortex

HUD   heads-up display

IFT   in-flight thrust (computer model)

INS   inertial navigation system

PLA   power level angles

WT   mass flow temperature

Symbols

A_{X_W} acceleration along the X-axis in the wind-axis coordinate system, ft/sec^2

b wingspan of F/A-18 airplane, 37.5 ft

C_D drag coefficient, $C_D = 2D/(\rho\, SV^2)$

C_{D_i} induced drag coefficient, $C_{D_i} = C_D - C_{D_0}$

C_{D_0} zero-lift drag coefficient

C_L lift coefficient, $C_L = 2L/(\rho\, SV^2)$

D drag, lbf

$F_{E_{DRAG}}$ engine throttle-dependent drag, lbf

F_{EX} excess thrust, lbf

F_G gross thrust, lbf

F_{RAM} ram drag, lbf

L lift, lbf

P power (engine), lbf-ft/sec

S wing area, ft^2

V velocity, ft/sec

W upwash velocity, ft/sec

W_G gross weight, lbm

WFT total fuel flow, lb/sec

X longitudinal separation (wingtip- to-wingtip), number of wingspans

Y lateral separation of wingtips, number of wingspans

Z vertical separation of wingtips (trail airplane relative to lead airplane), number of wingspans

Greek

α angle of attack, deg

γ flightpath angle, deg

θ pitch angle, deg

ρ density, lb/ft^3

Subscript

BL   baseline maneuver

est   estimated value

FF   formation flight

flight   flight-obtained value

lead   formation lead airplane

trail   formation trail airplane

INTRODUCTION

The performance benefits of flying an airplane in formation, known since before the advent of the airplane, have never been adequately quantified. The Autonomous Formation Flight (AFF) Project was conceived to demonstrate improved airplane performance by interacting with the vortex shed from the wingtip of a lead airplane. A goal of the project was to flight-test an autonomous system capable of maintaining formation position while flying in the dynamic flowfield of a vortex. After the performance benefits have been documented and understood, autonomous flight technology could potentially be applied to military formations, commercial cargo carriers, uninhabited combat aerial vehicles, and refueling tasks.

The initial phase of the AFF project demonstrated a prototype autonomous station-keeping system that was able to automatically control an F/A-18 airplane flying in formation. A position accuracy of about 4 ft was demonstrated while flying outside the influence of the wingtip vortex[1] of the lead airplane. The focus of this initial phase was the development and demonstration required of station-keeping technology to allow future clearance to fly autonomously within the vortex. Aerodynamic and control system data were obtained by the pilot manually holding formation position within the vortex. However, the aerodynamic and position feedback data obtained were inadequate to develop autonomous control laws and desired simulations.

To obtain the required data, it was necessary to document the influence of the wingtip vortex[1] of the lead airplane on the trail airplane. Improved knowledge of the vortex size, strength, and dynamics; the vortex influence on airplane handling qualities; and the influence of the vortex on vehicle aerodynamic coefficients[2] and performance were needed to reduce technology development risks. The AFF project performance goals included mapping the vortex effect on drag reduction and demonstrating improved fuel efficiency by at least ten percent. A critical requirement for achieving this goal was an accurate determination of engine and airplane performance for the trail airplane. The trail airplane was instrumented and analysis techniques were developed to obtain accurate thrust and drag values.[3] A position feedback system was installed on the heads-up display (HUD) to aid the pilot in acquiring this data.

This paper presents a summary of the AFF project vehicle performance benefits obtained during flight tests at the NASA Dryden Flight Research Center. This project recorded performance data at two flight conditions: the project design point, a Mach number of 0.56 and an altitude of 25,000 ft (condition 1); and a commercial transport flight condition, a Mach number of 0.86 and an altitude of 36,000 ft (condition 2). Drag and fuel-flow reductions for the trail airplane are presented. These reductions were obtained over a matrix of lateral, vertical, and longitudinal relative positions from the lead airplane. Contour plots map (1) the shape and intensity of the performance benefits and (2) the location of the optimum position within the vortex. Results revealed a time-averaged total-drag reduction of just over twenty percent and a time-averaged fuel-flow reduction of just over eighteen percent for the optimum formation position of the trail airplane. The effect of longitudinal position on performance benefits was also explored.

AIRPLANE AND ENGINE DESCRIPTION

Two NASA Dryden F/A-18 research airplanes were modified to support the AFF project. The F/A-18 airplane is a supersonic, high-performance, multimission fighter, powered by two F404-GE-400 turbofan engines each of which produce 16,000 lbf of thrust in afterburner. The engines are mounted close together in the aft fuselage. The F/A-18 airplane has a digital control-by-wire flight control system that provides excellent handling qualities. The airplane has a wingspan of 37 ft 5 in., a wing sweep of 20 degrees and a wing area of 400 ft.^{2} The fuselage is 56 ft long.

The AFF trail airplane (NASA 847) is a single-seat, F/A-18A airplane configuration that weighed 36,433 lbm when fully loaded with 10,860 lbm of internal fuel. The lead airplane (NASA 845) is a two-seat, pre-production airplane that has been extensively modified to conduct advanced flight systems research. Because it has a two-seat configuration, it carries less fuel and has a longer canopy. It weighed 36,021 lbm when fully loaded with 9926 lbm of fuel.

INSTRUMENTATION

Both F/A-18 airplanes were modified with global positioning system (GPS) receivers to provide precise relative-position information and generate vortex-mapping positioning cues for the pilot of the trail airplane. Each engine of the trail airplane was outfitted with a 20-probe turbine-exit total-pressure rake, fuel temperature probe, and volumetric fuel flow meter, which provided an accurate determination of engine thrust. The onboard computer of each airplane obtained standard airplane parameters, including Mach number, altitude, and gross weight. The inertial navigation system (INS) provided airplane rates and accelerations.

The standard production fuel-flow meter did not have the desired frequency response to accurately measure reduced fuel usage and calculate engine thrust while flying within the vortex. To accurately measure fuel flow during rapid throttle movements, a high-resolution, volumetric, fuel-flow meter was mounted on each engine of the trail airplane. These new research meters provided the desired improvement in dynamic response over the standard production meter. During steady throttle positions the research meter measured fuel flow to within 2 percent of the pre-existing production meter, which added confidence to the results. Reference 3 provides more information on the AFF performance instrumentation system.

FLIGHT TEST DESCRIPTION

Flight testing consisted of the trail airplane flying a matrix of test points relative to the lead airplane, over a grid of longitudinal, lateral, and vertical positions. The following sections describe the formation-flight coordinate system, the flight conditions tested, and the flight maneuvers conducted.

Formation Flight Coordinate System

The reference coordinate system used for longitudinal (X), lateral (Y), and vertical (Z) positioning of the trail airplane is shown in figure 1. Position location was normalized using the F/A-18 wingspan ($b = 37.5$ ft). The longitudinal separation was defined such that X is equal to 0 when both airplanes are

aligned nose-to-nose. Because the F/A-18 is 56 ft long, X is equal to 1.5 b when the nose of the trail airplane has zero separation distance to the tail of the lead airplane. The lateral position is defined such that when the wingtips are aligned, Y is zero; and when the wingtip overlap increases, Y has increasingly negative values. Vertical positions are defined such that when the wingtips are aligned, Z is zero; and when the trail airplane is below the lead airplane, Z is negative. As noted in the X-position conversion reference table in figure 1; longitudinal, lateral, and vertical positions discussed in this report will be referred to in units of wingspan.

Wingspan, b	Feet
0.0	0
1.5	56
2.0	75
3.0	113
4.4	165
6.6	248
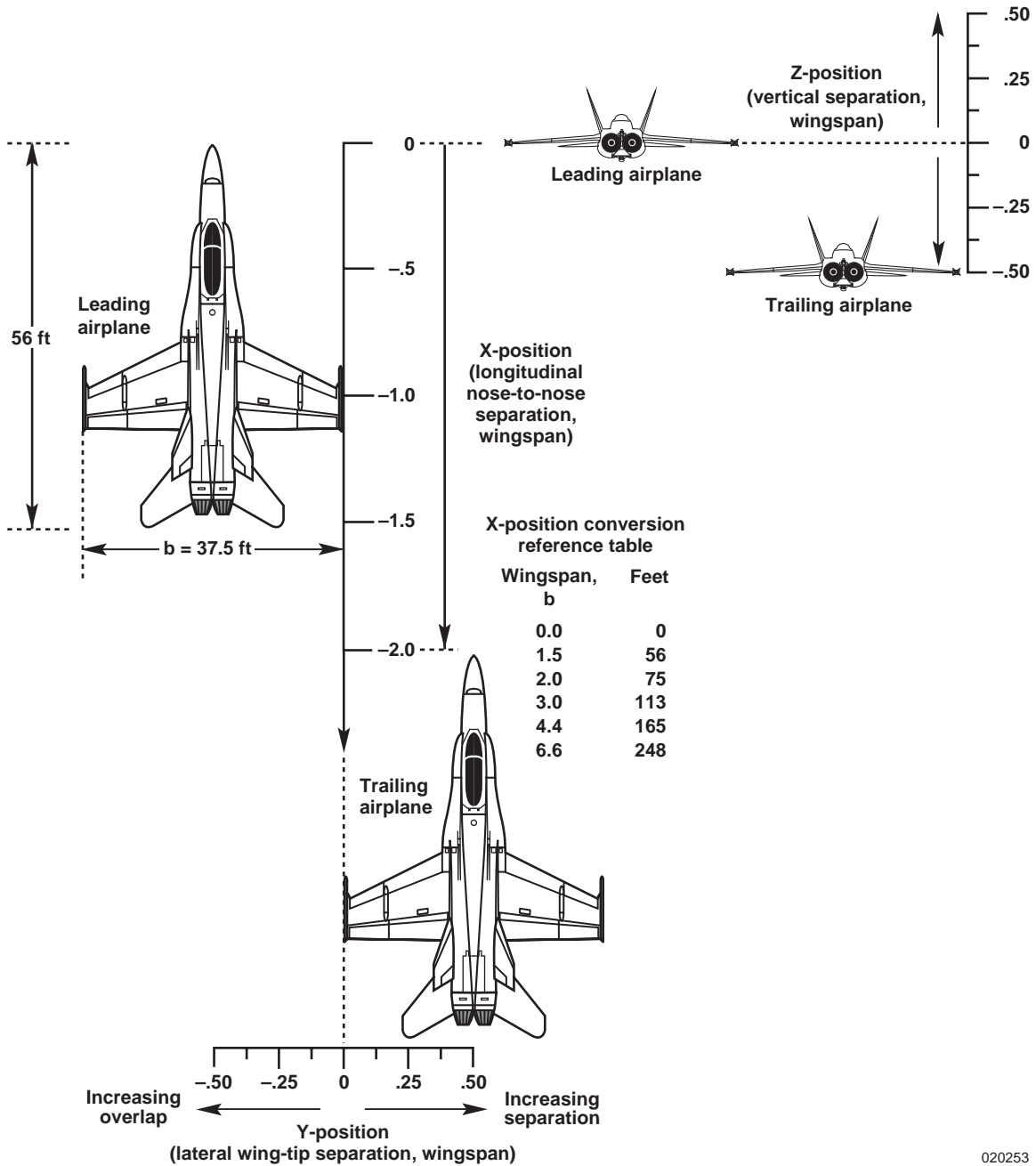
Figure 1. Autonomous Formation Flight Project, relative position coordinate system.

5

Flight Conditions Tested

The test point matrices were developed from predictions of aerodynamic and performance influences of a vortex on an F/A-18 wing and applied so that the maximum benefit of flying within the vortex would be near the center of each matrix. The test points were flown at two flight conditions: condition 1 (at a Mach number of 0.56 and an altitude of 25,000 ft); and condition 2 (at a Mach number of 0.86 and an altitude of 36,000 ft). Most of the flight research obtained was conducted at condition 1, which was chosen to match predicted data previously produced by The Boeing Company (Long Beach, CA). Condition 2 was aimed at exploring the regime of commercial transports. The initial Y-Z grid was chosen such that increments equaled one-eighth of a wingspan or 4.7 ft. To explore the effect that longitudinal position (X) has on the vortex influence, the Y-Z matrix of test points was flown at four trailing locations. At both flight conditions, substantial data was obtained at X positions of 3.0 b and 4.4 b, the former position being the primary test matrix. Additional data was acquired at X positions of 2.0 b, 6.6 b, and further aft to determine how far aft the influence of the vortex existed.

Figure 2 provides a summary of the test points planned and flight-tested at condition 1. Open symbols were not flown, either because trends in the flight-data obtained showed little performance benefit or because of limitations in the flight schedule. The largest number of test points flown at both flight conditions was at an X position of 3.0 b, followed by the 4.4 b and 6.6 b positions. Because of safety concerns, the test points at the closest trailing positions from the lead airplane ($X = 2.0$ b, or 20 ft nose-to-tail separation) were limited to the amount of wing overlap needed to assure adequate separation in the event the lead airplane experienced an engine failure.

As the flight test program progressed and the optimum Y-Z location became more apparent, additional test points were added to further define the test-point matrix grid. These test points identified the vortex location more precisely, to find the optimum formation position location that would yield the maximum performance benefit. In addition, once the optimal Y-Z position was determined, a series of test points were conducted at various X positions to gather more data on the effect of longitudinal position on formation performance.

A similar airplane-position matrix of data was obtained at condition 2. No additional finer-grid data was obtained at this condition.

Flight Test Maneuvers

Each test point consisted of two separate flight maneuvers. The first maneuver was formation-flight station keeping (FF) within the influence of the wingtip vortex shed from the lead airplane. The second maneuver was non-formation cruise, at the same flight condition previously flown within the vortex. This maneuver was called the baseline maneuver (BL). When the target flight condition was attained, the following sequence of events defined an ideal test point. First, the trail airplane held the X, Y, and Z positions within the vortex for 30 seconds of steady data. Next, the automatic-throttle control (ATC) was engaged while maintaining position within the vortex for 20 additional seconds of steady data, with minimal changes in throttle position and airplane velocity.
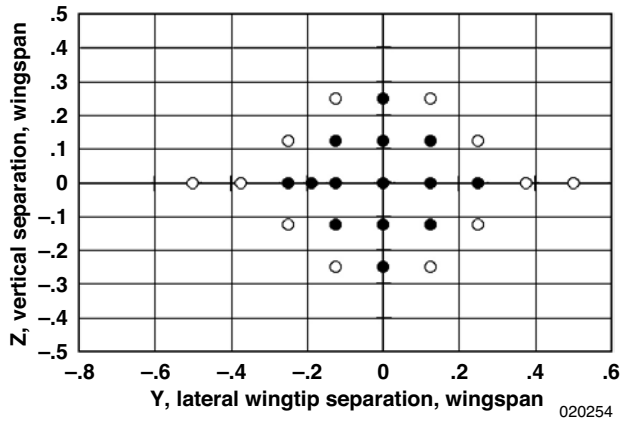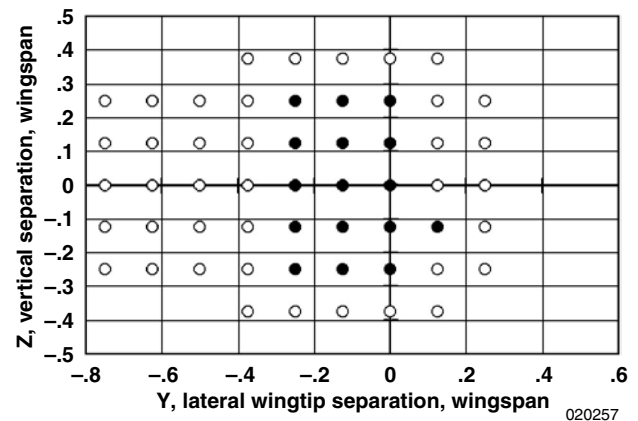
(a) $X = 2.0\ b$
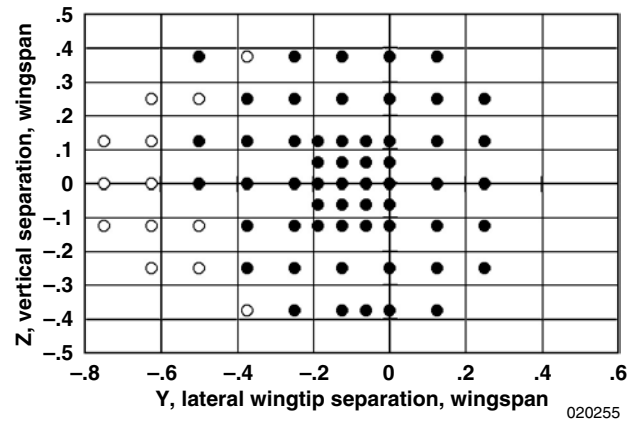
(b) $X = 3.0\ b$
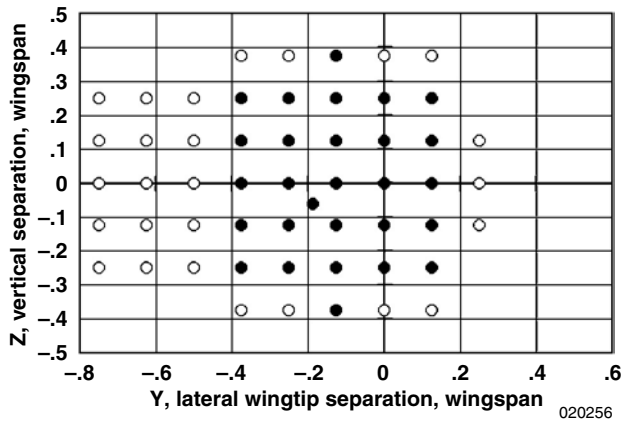
(c) $X = 4.4\ b$

(d) $X = 6.6\ b$

Figure 2. Performance test points flown for various longitudinal (X) positions at condition 1.

Finally, with ATC still engaged, the trail airplane engaged altitude-hold, then laterally slid away from the lead airplane (performed a slide-out maneuver), and stabilized outside of the vortex for 30 seconds of baseline data. This technique provided airplane performance data within the vortex, followed immediately by baseline data, from which changes in airplane performance could be readily determined. Figure 3 provides a good example of the calculated drag change during a test point, as the trail airplane moves from FF to BL. Also shown is the predicted drag coefficient, calculated using the Dryden Digital Performance Simulation (DPS).[4] As demonstrated, the airplane drag coefficient is reduced by over 20 percent while in the vortex, and returns to the predicted value when moved away from the influence of the vortex.
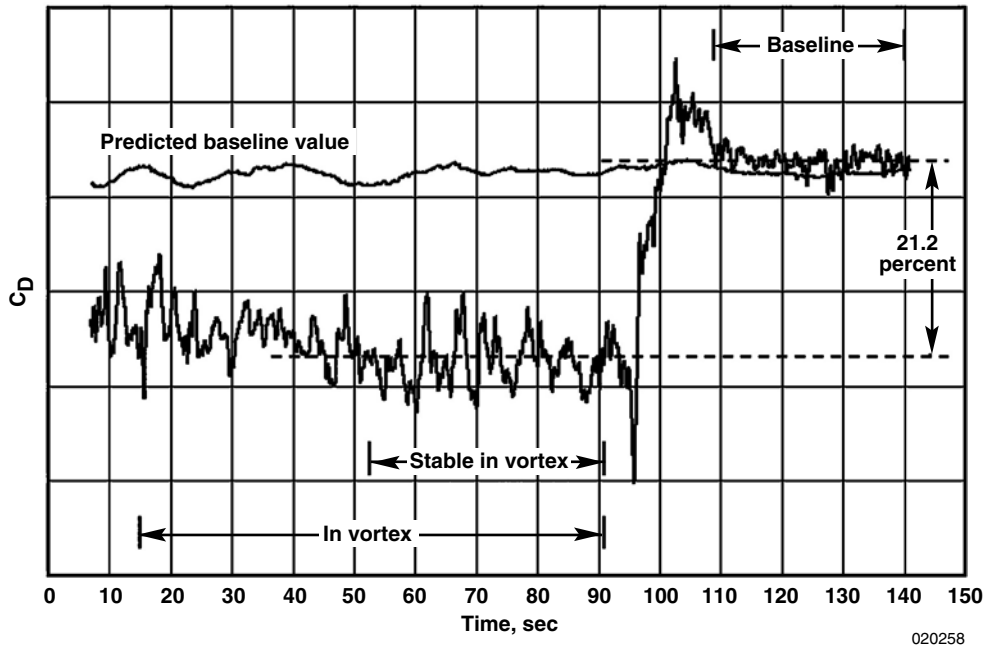
7

Figure 3. Example drag change during a test point at condition 1, $X = 4.4\,b$, $Y = -0.17\,b$, and $Z = -0.05\,b$.

The initial 30 seconds of data were required to estimate hinge moments on the control surfaces that were necessary to maintain stable flight within the influence of the vortex.[2] The next 20 seconds of data, with ATC engaged, were used to determine the drag coefficient and to measure the fuel flow while flying within the vortex. By engaging ATC, both throttles were set to equal power level angles (PLA) and the digital engine control computer maintained indicated airspeed by changing the PLA. When engaged, the computer constantly made small adjustments in PLA, resulting in decreased amplitude and decreased frequency of throttle inputs over the span of a test point than when the throttles were moved manually. The final 30 seconds of stable data, well outside of any vortex influence, were needed to calculate baseline drag values. When transitioning from FF to BL, the automatic-throttle system automatically responded to changes in drag after the slide-out, which resulted in an increase in fuel flow to maintain speed.

The quality of data obtained at each test point was a function of airplane handling qualities. With over one minute of steady flight required at each test point to successfully calculate airplane performance, it was common to encounter atmospheric upsets or for the airplane to drift off of particular flight conditions. Many test points were repeated to verify drag- and fuel-flow-reduction values obtained previously, in order to build confidence in the data. Points with a large amount of wing overlap were often too unstable for the pilot to stay on conditions for more than a few seconds at a time, which resulted in poor data quality. Further discussion on data quality is provided in reference 3.

ANALYSIS METHODS

To show the benefits of flying within the vortex, an accurate determination of engine and airplane performance was required. Airplane performance was determined using classical techniques and a computational model. Reference 3 presents a comprehensive discussion of the analysis techniques used to obtain the airplane and engine performance data.

In-Flight Thrust Model

The manufacturer's in-flight thrust (IFT) model for the F404-GE-400 engine was used to calculate accurate thrust values for each engine. The basic model uses two correlation techniques for determining ideal gross thrust: area pressure (AP) and mass flow temperature (WT). The WT technique was chosen as the method for calculating engine performance because of its proven accuracy, which was close to 2-percent for net thrust.[5] The model calculated gross thrust (F_G), ram drag (F_{RAM}), and engine throttle-dependent drag ($F_{E_{DRAG}}$). Gross thrust is the primary force the engine produces at the turbine exit station without any other effects or losses; F_{RAM} represents the force resulting from or caused by the momentum of air entering the inlet; and $F_{E_{DRAG}}$ accounts for the external drag forces associated with the engine nozzle and inlet spillage flow. The IFT model also accounts for the F/A-18 installation effects of bleed air and horsepower extraction.

Airdata and Aircraft Model

In addition to standard calculations such as Mach number, altitude, and gross weight, the airdata and aircraft model included a calculation for an estimated angle of attack, α_{est}, which is based on the pitch angle of the trail airplane and the flightpath angle of the lead airplane ($\alpha_{est} = \theta_{trail} - \gamma_{lead}$). Angle-of-attack probes for the trail airplane were unusable during formation flight because of localized influences of the vortex and the upwash generated from the lead airplane. Because the lead airplane flew at steady-state conditions (constant speed and altitude, barring turbulence), the flightpath angle, γ_{lead}, was always close to zero.

Inertial Navigation System-Acceleration Correction Model

The INS was used to obtain vehicle acceleration data. These data were corrected for rotation effects, as the INS was not mounted exactly at the center of gravity. The data were then translated into the flightpath (wind axis) coordinate system. Axial acceleration was used to compute vehicle excess thrust $F_{EX} = W_G \times A_{X_W}$.

Vehicle Performance Models

This program used two versions of the AFF vehicle performance model. The first model was a simplified real-time version used during flight-testing. The second model was a more sophisticated version that contained postflight corrections for various sources of error, including atmospheric effects and INS offsets.

Real-Time Model

Real-time calculations used a simplified thrust and performance algorithm installed on a workstation in the Dryden mission control center. This approach was successfully demonstrated on past flight programs such as X-29, F-18 HARV, and X-31.[5] Displays showed parameters calculated by the real-time algorithm for the duration of every flight. This information served to monitor the status of critical instrumentation, to determine the quality of test points performed, and to evaluate gross estimates of the vortex effects on the trail airplane. Performance trends were easily identifiable using time histories of the real-time data. Test points that appeared to be of particular value to the project could be repeated or investigated in-depth. This was particularly true when obtaining FF data near the optimum location of the vortex and obtaining BL data immediately after.

Postflight Model

The postflight performance model used the INS-corrected data to obtain lift, drag, and respective coefficients for the trail airplane. To calculate drag reduction values, data obtained during FF was compared with BL data that had been completed in consecutive fashion to minimize uncertainty. Some test points did not include a slide-out maneuver to obtain BL data. For these few points, BL data were estimated based on data trends in drag coefficient as a function of gross weight.

Performance data were determined using classical techniques. A balance of forces perpendicular to the flightpath was used to determine lift. A summation of forces along the flightpath was used to determine drag:

$$D = \cos(\alpha_{est})F_G - F_{RAM} - F_{E_{DRAG}} - W_G \times A_{X_W} \tag{1}$$

The drag change for formation flight was determined by comparing drag of the trail airplane while in FF to its BL values as follows:

$$
\begin{aligned}
\text{Percent drag reduction} \\
= \Delta D / D_{BL} \\
= (D_{BL} - D_{FF})/D_{BL} \\
= 1 - (D_{FF}/D_{BL})
\end{aligned}
\tag{2}
$$

Simplified Performance Simulation Model

A simple prediction model, the Dryden digital performance simulation (DPS), calculated lift and drag predictions for the F/A-18 airplane using processed flight data. These predicted values were used to compare and verify the drag values obtained during FF and BL maneuvers.

RESULTS AND DISCUSSION

The AFF program demonstrated significant performance benefits. For the optimum FF position of the trail airplane, results showed a time-averaged total-drag reduction of just over 20 percent and a time-averaged fuel-flow reduction of just over 18 percent. Data variability, which affected the consistency or quality of the data, was primarily a result of the range-of-difficulty that pilots encountered trying to hold each specified relative position behind the lead airplane. An in-depth discussion defining data quality for this program is in reference 3. Several positions were highly unstable, particularly those with large overlaps in wing position ($Y < -0.3\ b$). In certain positions, the instability was exaggerated when the wingtip vortex of the lead airplane impinged directly on the vertical tail of the trail airplane. When the vortex was outboard of the trailing airplane wing (positive wingtip separations), the data tended to be more consistent and better quality than the inboard data. This was primarily a result of reduced vortex influence on the controllability of the airplane. The region of best drag benefits was fairly stable throughout, and good data quality was obtained during most points. It is believed that the drag reduction and fuel savings could be increased if control of the two formation airplanes is provided by a more precise autonomous formation flight system, which is still in development.

A relatively coarse map of the vortex was able to identify a large region of performance benefits for the trail airplane. These results helped identify two key drivers for the development of an autonomous formation flight control system. First, the data identified the required precision that must be maintained by the positioning coordinates of the trail airplane to stay within the beneficial influence of the vortex. The precision of maintaining the trail airplane position affects the gains used for control surfaces inputs. Second, the data identified the dissipation of the strength of the vortex downstream of the lead airplane. The rate at which the vortex dissipates affects how rigorously the throttle must be moved to maintain axial position behind the lead airplane before performance benefits become negligible. In close formations, the trail airplane may use more fuel during a mission because the pilot is constantly adjusting the throttles to maintain a precise visual position relative to the lead airplane. Continuous throttle movement puts the engines in a rapid cycling of "spool-up" and "spool-down" during tight formation flight, resulting in a notable increase in fuel flow. Control laws developed for autonomous station-keeping need to consider minimizing throttle changes to maximize performance benefits.

The changes in lift and drag coefficient were evaluated for each test point by comparing the FF to BL values. In general, very small changes (differences of less than 2 percent in average lift coefficient, in and out of the vortex) were found for all positions of the trail airplane. Figure 4 shows this trend, in which the ratio of flight lift coefficient to the DPS-estimated lift coefficient ($C_{L_{DPS}}$) are plotted. In this figure, lift coefficient (C_L) fluctuates as it is influenced by the vortex within a band of ±5 percent of the estimated $C_{L_{DPS}}$, yet its average value in the vortex is close to the average value outside of the vortex.
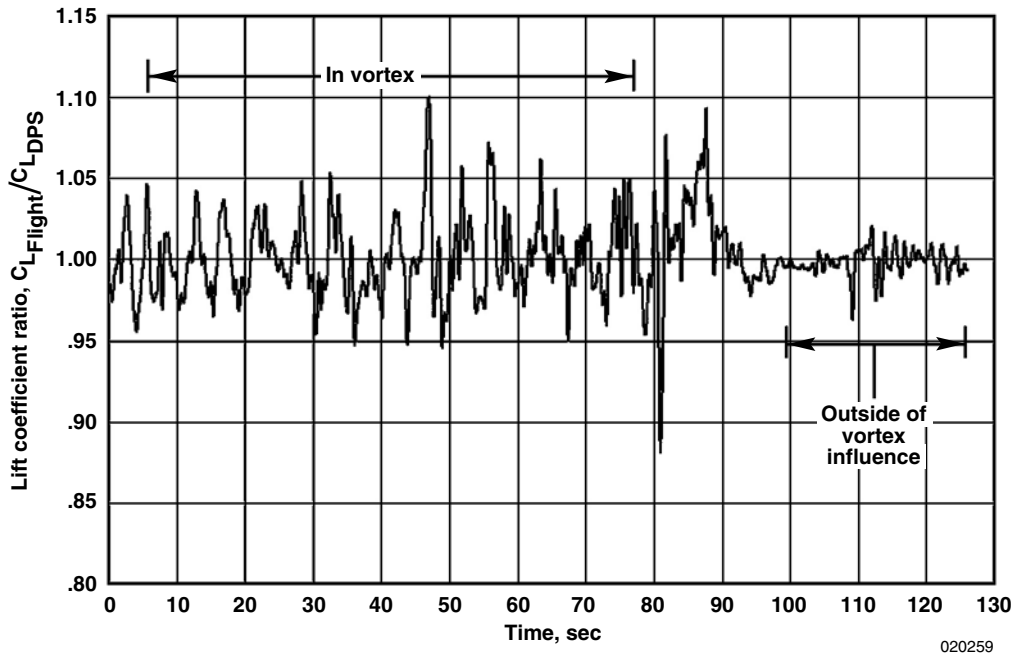
Figure 4. Example lift coefficient change during a test point at condition 1.

Data Uncertainty

The uncertainty in the calculated C_D was estimated to be on the order of five percent. The flight test technique of comparing calculated drag coefficient in formation flight, $C_{D_{FF}}$, to that of the baseline condition, $C_{D_{BL}}$, minimized any bias effects. Several additional factors influenced the final uncertainty of the data. These factors include variations in maneuver technique, air turbulence, stability of the vortex location, and the accuracy of the position measurement system.

Another important factor was the effect that airplane weight changes had on the vortex strength of the lead airplane and on the absolute drag value calculated for the trail airplane. Depending on whether a test point was conducted near the beginning or the end of a flight, the differences in airplane weight, because of fuel burn, changed the aerodynamic trim characteristics of both the lead and trail airplanes. No corrections for trim drag effects were made. Time-averaging the data and repeating several test points helped improve the overall quality of the results. However, the final uncertainty is difficult to fully assess because these factors discussed are difficult to quantify.

The following sections discuss the detailed vehicle performance results obtained for total drag, induced drag, and fuel flow at the two primary flight conditions. The optimum position for each performance parameter is discussed and the effects of longitudinal separation are summarized.

12

Improvement in Total Drag

The calculated drag reductions for two flight conditions and four longitudinal stations are presented in figures 5 and 6. These figures show the percentage of change in airplane drag coefficient from baseline, as a function of lateral and vertical separation. Figure 5 presents the flight results obtained at flight condition 1 while figure 6 presents the data obtained at flight condition 2.

Figures 5 and 6 show this data as a function of lateral spacing (wing overlap) in a line-plot format at various vertical offsets and longitudinal positions. These plots provide the exact data gathered during the AFF flight program. Figure 7 shows the same data as figures 5 and 6, but is interpreted using a bicubic spline contour plotting routine in Matlab. This provides a valuable two-dimensional image of the size and magnitude of the vortex-induced benefits at each flight condition, based on vertical and lateral position. To allow direct comparisons, these contour plots show equivalent Y-Z ranges, resulting in blank areas where data was not gathered. It is important to stress that these plots are interpolations of a limited number of flight data points and the nature of the interpolation routine and inaccuracies at individual data points could lead to misinterpretations of details. In general though, they provide a valuable illustration of the vortex effect on drag reduction.

## Flight Condition 1: Mach number 0.56 at an altitude of 25,000 ft

At condition 1 and $X = 3.0$ b, over 20 percent drag reduction was calculated on several test points. The complete data set at this longitudinal station is shown in figures 5(b) and 7(a). Many of these large reductions were obtained from the test points flown at a vertical separation of $Z = 0.06$ b. These test points were added during the flight program to help refine the location of best drag reduction, as mentioned previously. Peak values are between a vertical position of $–0.13$ $b < Z < 0.0$ b and a lateral position of $–0.2$ $b < Y < –0.1$ b (wings overlapped). A large region of substantial benefits was found, with drag reductions greater than 10 percent for a region between separation $Z = 0.10$ b to $–0.25$ b vertical separation and a lateral range of almost $Y = –0.30$ b to 0.05 b.

At the longitudinal position $X = 4.4$ b, similar results were demonstrated as shown in figures 5(c) and 7(c). Over 20 percent drag reduction was calculated at two test points with the peak reductions ranging between $–0.05$ $b < Z < 0.05$ b vertical position and a lateral position of $–0.20$ $b < Y < 0.05$ b. At this longitudinal station, the peak value is located approximately at zero vertical separation, or wings-aligned. This differs slightly from the $X = 3.0$ b station, where the peak values were calculated to be several feet below wings-aligned. While the peak drag reduction is similar to that at the $X = 3.0$ b position, the region of substantial benefit is smaller and the gradient from performance benefit to detriment is not as steep at the inboard test points.

At $X = 6.6$ b, a reduced matrix of test points was investigated. The available data in figures 5(d) and 7(e) show a calculated drag reduction up to 18.7 percent obtained between $–0.20$ $b < Y < –0.10$ b and a vertical position between $–0.15$ $b < Z < –0.10$ b. The trend in the data indicates that the actual peak at this station may not have been identified with the available data, and may in fact be located slightly further inboard. However, the available data does allow for the selection of a singular peak position, as it is the only test point with a calculated drag reduction above 15 percent. This location is $Y = –0.126$ b and $Z = –0.125$ b. When plotted in the contour format, the peak is virtually indiscernible from the trends in the other data points. This can likely be attributed to the continuous vertical and lateral translation of the vortex, or wandering, identified by the project pilots as well as by the limited data set.
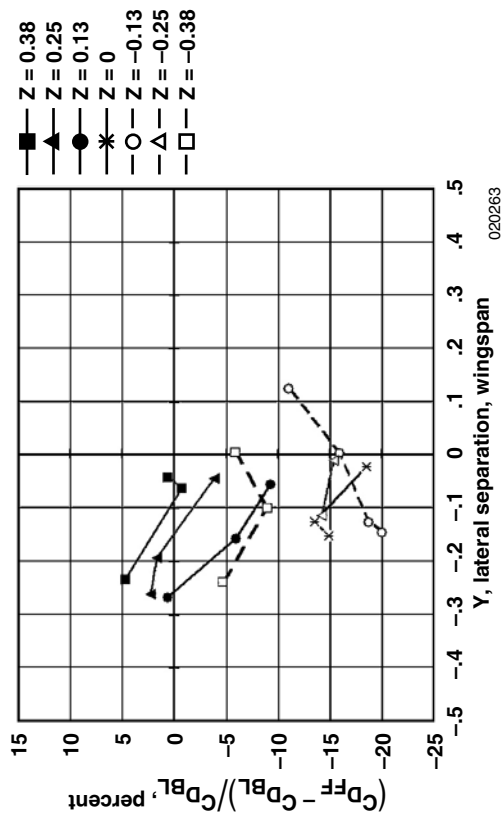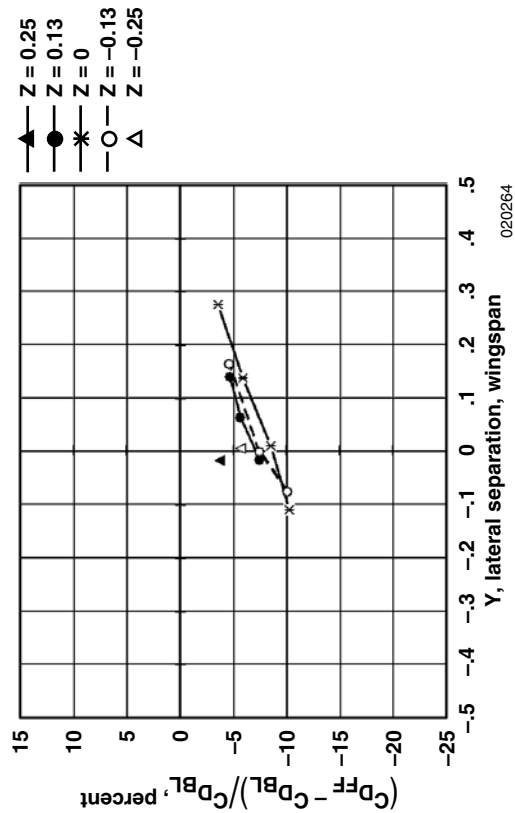
13
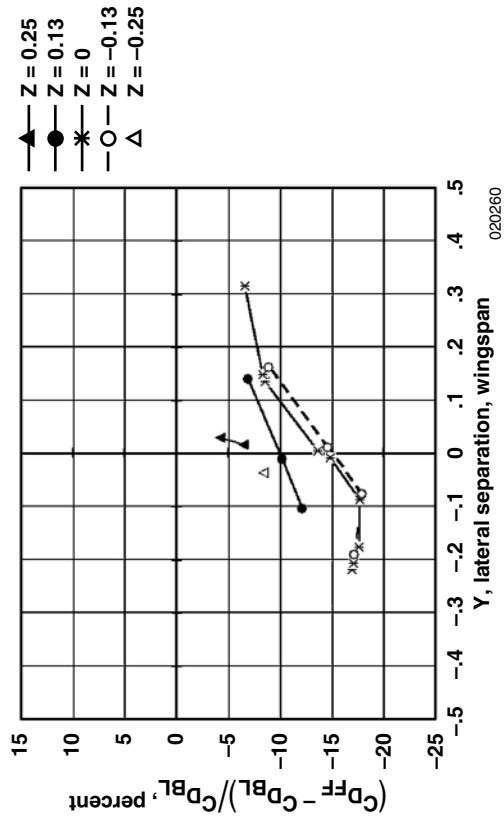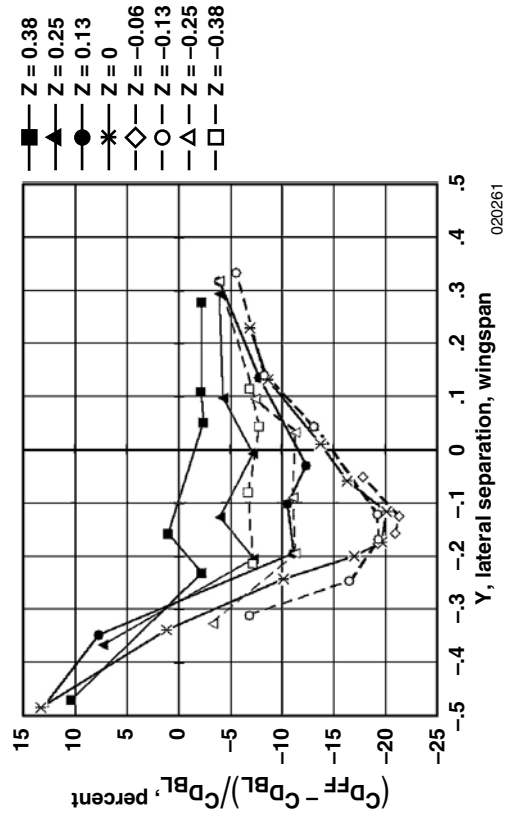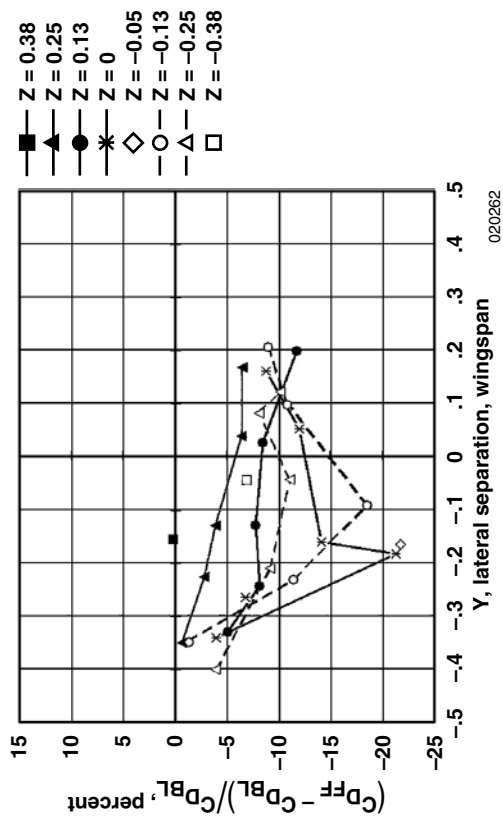
Figure 5. Demonstrated drag change on the trailing airplane in formation flight at condition 1, four longitudinal separations
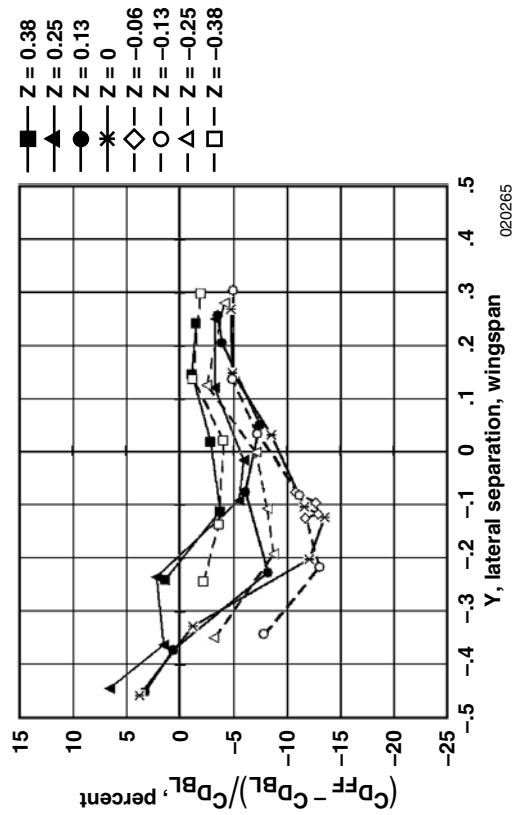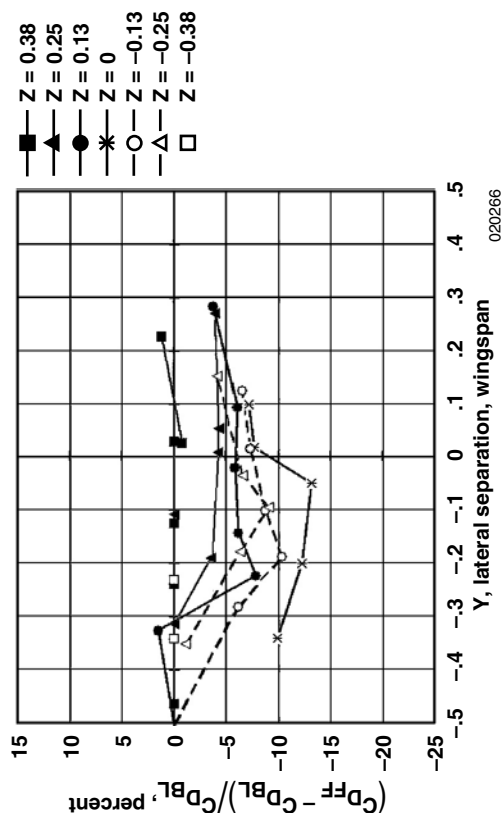
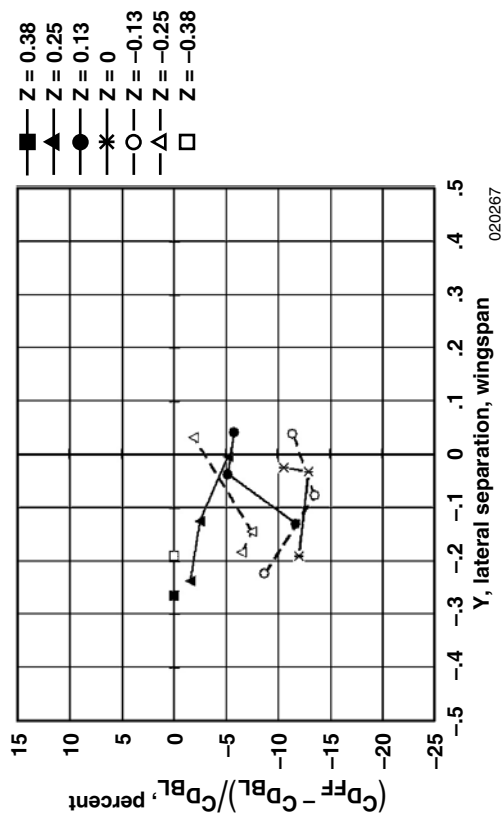Figure 6. Demonstrated drag change on the trailing airplane in formation flight at condition 2, four longitudinal separations.
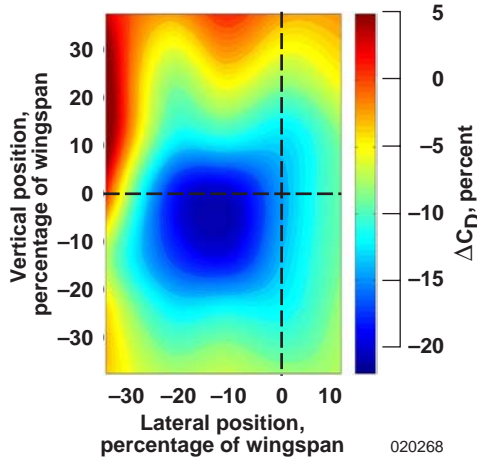
(a) $X = 2.0\,b$
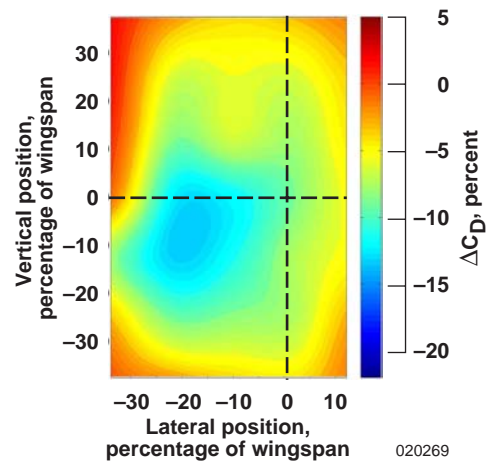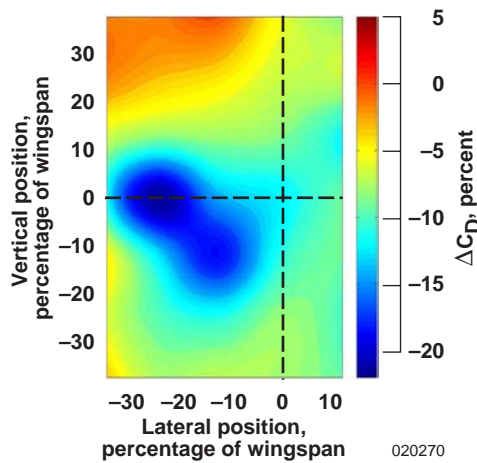
(b) $X = 3.0\,b$

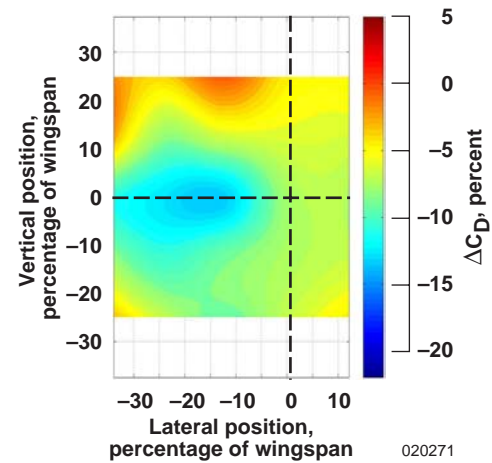(c) $X = 4.4\,b$

(d) $X = 6.6\,b$
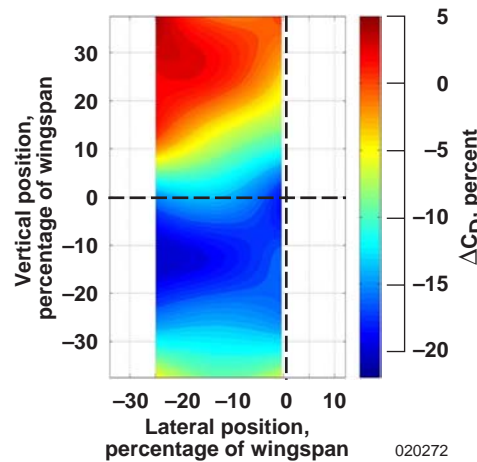
(a) $X = 3.0\ b$, condition 1
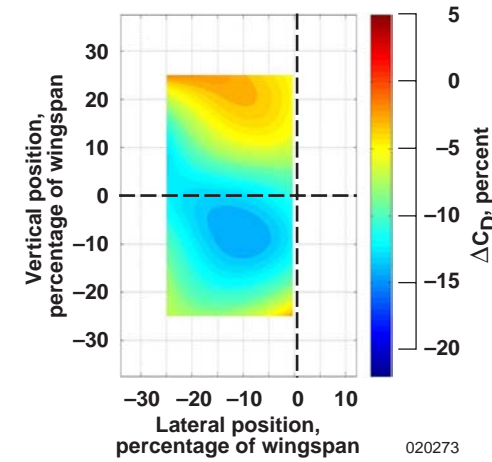
(b) $X = 3.0\ b$, condition 2

(c) $X = 4.4\ b$, condition 1

(d) $X = 4.4\ b$, condition 2

(e) $X = 6.6\ b$, condition 1

(f) $X = 6.6\ b$, condition 2

Figure 7. Summary of drag (C_D) reduction contour plots as a function of Y-Z position at conditions 1 and 2.

16

At $X = 2.0\ b$, aerodynamic instabilities resulting from airframe interaction with the vortex prevented the pilots from maintaining steady flight at many of the desired test points. Eighteen successful test points were flown at and around the perceived region of most benefit, and in figure 5(a), the results are comparable to those at the other three stations. Drag reductions of almost 18 percent were calculated at vertical offsets of $Z = 0.0\ b$ and $-0.125\ b$ and within $Y = -0.20\ b$ to $-0.05\ b$. Even with a limited data set at this station, these results are quite comparable in terms of magnitude and offsets to the other three stations. All test points were controllable by the pilots and quasi-steady with an elevated pilot workload in comparison to the other three longitudinal stations.

At the four longitudinal positions studied, it was demonstrated that the downstream degradation in the vortex is minimal, and nearly 20 percent drag reduction can be achieved at all four longitudinal stations. Table 1 presents a summary of the drag reduction values and the optimal locations at all flight conditions and longitudinal stations. From this summary data, the approximate optimal location at condition 1 varies at lateral stations from $Y = -0.05\ b$ to $-0.20\ b$ and vertical stations from $Z = 0.0\ b$ to $-0.125\ b$. Additional test points were flown at and around this optimal location at $X = 3.0\ b$, repeatedly verifying the reduction in drag of over 20 percent.

Table 1. Summary of drag, fuel-flow reductions, and optimum position results at condition 1.

		Mach number 0.56 at an altitude of 25,000 ft			
X - Position, b (ft)		0.5 (20)	1.5 (55)	3.0 (110)	5.0 (190)
Maximum Reduction, percent	C_D	18	21.3	21.7	18.7
	C_{D_i}	40	49	42	46
	WFT	14[*]	18.6	18.6	18.7
Optimal separation position, b	Lateral, Y	−0.18 to −0.08	−0.122	−0.174 −0.122	−0.20 to −0.10
	Vertical, Z	−0.125 to 0.0	−0.06	0.0 to −0.13	−0.15 to −0.10
Number of data points		20	92	42	21

* Only one measured fuel reduction for 20 ft, at condition 1.

Flight Condition 2: Mach number 0.86 at an altitude of 36,000 ft

When comparing figures 7(a) and 7(b), the contour plot presenting drag reduction at condition 2 and $X = 3.0\ b$ is similar in cross-sectional shape to condition 1, but lower in overall magnitude. The maximum drag reduction was about 13 percent. Similar to the results at condition 1, the best performance improvements occurred when the trailing airplane was laterally at an inboard station from wingtips aligned, $Y = -0.10\ b$ to $-0.25\ b$, and vertically between $Z = 0.0\ b$ to $-0.125\ b$. This lower drag benefit is primarily a result of the airplane operating at a lower ratio of induced drag to total drag. Flight test results that demonstrate the real-world effect of formation position and flight conditions on C_{D_i} will be presented in the "Improvement in Induced Drag" section of this report.
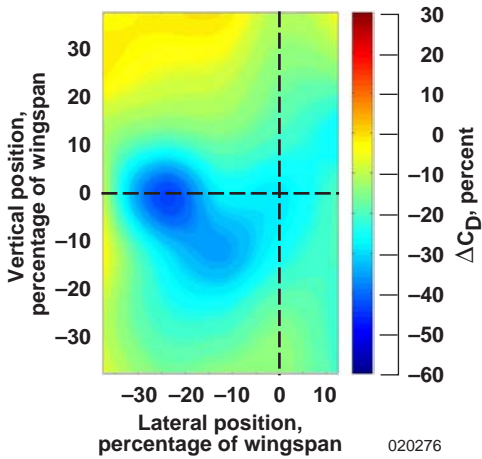
At $X = 4.4\ b$, a drag reduction of just over 13 percent was demonstrated. This is shown in figures 6(c) and 7(d). Within the uncertainty of this analysis, this result is nearly equivalent to the maximum drag reduction demonstrated at $X = 3.0\ b$. In comparing figures 8(c) and 8(d), the most notable difference
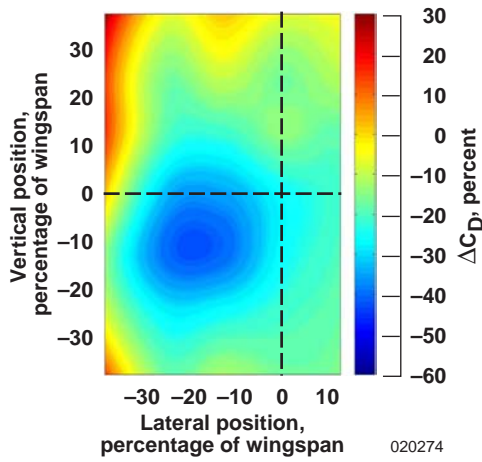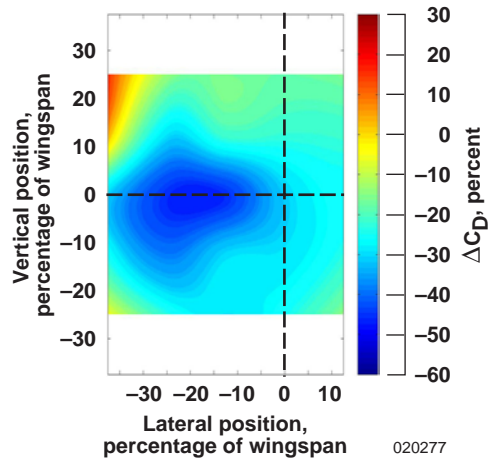
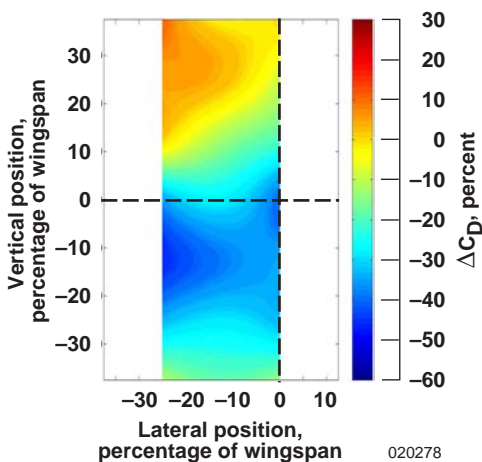(a) $X = 3.0\ b$, condition 1
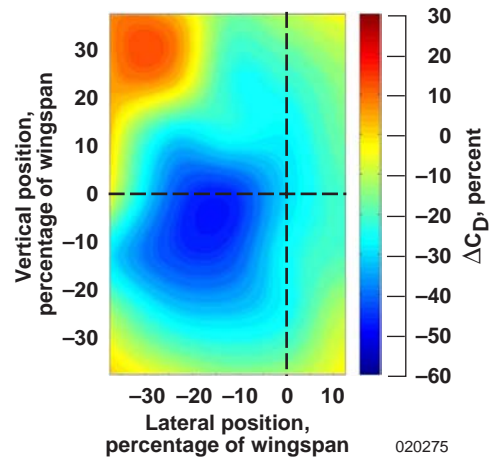
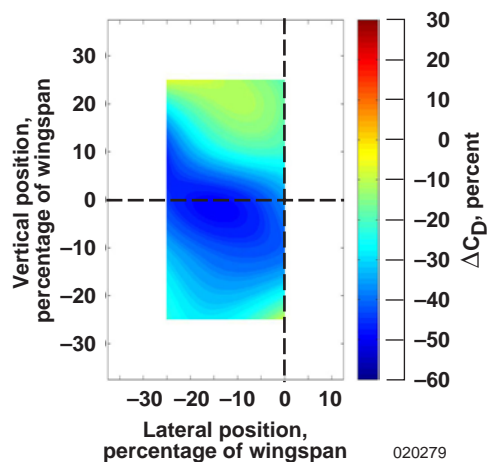(b) $X = 3.0\ b$, condition 2

(c) $X = 4.4\ b$, condition 1

(d) $X = 4.4\ b$, condition 2

(e) $X = 6.6\ b$, condition 1

(f) $X = 6.6\ b$, condition 2

Figure 8. Summary of induced drag (C_{D_i}) reduction contour plots as a function of Y-Z position at conditions 1 and 2.

between this data and that obtained at condition 1 (other than overall magnitude) is the gradient in drag reduction. At this increased altitude and Mach number, the change in drag reduction is much more gradual as a function of lateral and vertical position.

As shown in figures 6(d) and 7(f), at $X = 6.6\ b$, the region of most benefit shifted noticeably to a more outboard (greater Y value) location than at $X = 4.4\ b$ to a region between Y= –0.05 and –0.15 wing overlap. This region is vertically located between an offset of $Z = \pm0.05$. The largest drag reduction was calculated to be 13.5 percent. The gradient in the drag reduction magnitude as a function of lateral and vertical position appears to be consistent with the other two longitudinal stations at this flight condition discussed thus far.

At $X = 2.0\ b$, drag reductions of 10 percent were calculated at vertical stations of $Z = 0.0\ b$ and –0.125 b and a lateral range of approximately Y= –0.05 b to –0.11 b. Data to support this conclusion is presented in figure 6(a). These ranges are consistent with the results obtained at this station at condition 1 and the peak magnitude is comparable to the results at the other three stations.

However, insufficient data was gathered to determine whether the actual peak in drag reduction was observed. As at the other condition 1, all test points were controllable by the pilots, quasi-steady, with an elevated pilot workload compared to the other three longitudinal stations.

Table 2 shows a summary of the peak drag values and optimal locations at this flight condition. From this summary data, the approximate optimal location at condition 2 varies between lateral stations from $Y = 0.0\ b$ to –0.25 b and vertical stations from $Z = 0.0\ b$ to –0.125 b. When compared to the results at condition 1, this region is shifted slightly outboard by 0.05 b, but within the same vertical bounds.

Table 2. Summary of drag, fuel-flow reductions, and optimum position results at condition 2.

		Mach number 0.86 at an altitude of 36,000 ft			
X - Position, b (ft)		0.5 (20)	1.5 (55)	3.0 (110)	5.0 (190)
Maximum Reduction, percent	C_D	10.2	13	13.2	13.5
	C_{D_i}	42	46	45	48
	WFT	n/a	12.2	16.5	14.6
Optimal separation position, b	Lateral, Y	–0.11	–0.21	–0.05 to –0.20	–0.15 to –0.05
	Vertical, Z	0.0	–0.125 to 0.0	0.0	–0.05 to 0.05
Number of data points		12	51	34	16

Range of optimum positions indicated best reductions obtained.
No slide-outs were performed for 20 ft, at condition 2.
No data obtained below Y = 11 percent at 20 ft, at condition 2.

Comparing all six contour plots (fig. 7), additional trends become apparent. The cross-section of the vortex, in terms of its potential for drag reduction, is circular at a longitudinal separation of $X = 3.0$ b, for both flight conditions. At $X = 4.4$ b, the cross-section is still well defined, but more oval-shaped or elliptical at both flight conditions. At $X = 6.6$ b, the data provides a broadly distributed cross-section without notable definition at condition 1, appearing to confirm the pilots' perception that the vortex position is not fixed at longitudinal positions further aft. Even with these noted changes in the shape and intensity of the vortex at different flight conditions, optimal drag benefits (greater than 10 percent drag reduction) are apparent at all longitudinal stations and all flight conditions within a vertical position of wings aligned to $Z = –0.10$ b and a wing overlap of $Y = –0.10$ b to $–0.25$ b. This is a consistent and generous region (21 ft)^2 to work with from the standpoint of an autonomous station-keeping control system. It has been demonstrated that the pilot or control system requires only a low precision in lateral and vertical accuracy for maintaining relative position within this beneficial region.

Even at separations of $X = 6.6$ b, data averaged during the in-vortex and baseline maneuvers of a test point demonstrated significant gains, both calculated and measured, while in the vortex. At the more distant longitudinal stations, the amplitude of measured performance parameters varied greatly while in the vortex, almost in a cyclic nature, but the average values show benefits of consistent magnitude with the other stations. The cyclic nature of the measurements is further evidence that either the vortex wandered around at these stations or the pilot was constantly maneuvering to chase what was believed to be the location of the vortex. This is a phenomenon that station-keeping technology could not fully exploit unless it continually sought to find the peak.

The data is not symmetric about the peak position and, as expected from theory,[6-10] all data show more sensitivity (steeper gradients) as the trailing airplane moves inboard compared to the outboard positions. This is because the upwash changes to a downwash as the trailing airplane passes through the vortex center while moving inboard. In fact, significant drag *increases* were measured at some high-wing overlap positions, verifying the importance of proper station-keeping to obtain the best results.

Improvement in Induced Drag

A finite wing generates vortices at the wingtips as a result of upper and lower surface pressure differences inherent to a lift-generating device. The wingtip vortices contain a large amount of translational and rotational kinetic energy. This energy is ultimately provided by the airplane engine, which is the only source of power associated with the airplane. Since the energy of the vortices normally serves no useful purpose for an airplane flying solo (not in formation), this energy is essentially lost to viscous effects as it dissipates into the air. In effect, the extra power provided by the engine that goes into the vortices is the extra power required by the engine to overcome this drag force, termed "induced drag".[11] By interacting with the lead airplane vortex, the AFF project was able to demonstrate a great reduction in the induced drag of the trail airplane, which can be translated into a reduction in power-setting required to fly the same mission as the lead airplane.

Induced drag, C_{D_i}, was also calculated to allow for comparison to basic prediction theory.[3,6-10] Although several sources of predictive data are available, the simplest theoretical analysis for predicting drag reduction while in formation flight replaces each wing with a single "horseshoe" vortex. With this analysis, an assumption is made that only the induced drag (not form drag), C_{D_i}, is affected by the upwash influence. These predictions also assume that the percentage of change in induced drag is unaffected by flight condition. Thus, for a given percentage of reduction in C_{D_i}, a larger percentage of change in C_D will be obtained at condition 1 than at condition 2. Hoerner predicts that a single trailing

aircraft can have an induced drag reduction of 40 percent when flying one wingspan aft of the lead (nose-to-nose separation) at zero vertical and lateral separation.[9]

Results from the AFF program show peak reductions in induced drag approaching 50 percent for all flight conditions and longitudinal stations. Contour plots representing the percentage of change in calculated induced drag as constant-value isolines are shown in figure 8 for the flight data available. Although the magnitudes are significantly larger, the shapes and gradients of these plots closely resemble the contour plots of total drag data discussed previously. Comparing the plots as a function of flight condition, the reductions are notably more dramatic at condition 2, where increased regions of induced drag reductions of 40 percent or greater were calculated. This effect is contrary to the assumptions made in the basic prediction theories of references 3 and 6–10, which imply that changes in induced drag for formation flight should be independent of flight condition. Uncertainty in the flight data could account for the differences in C_{D_i} reductions obtained at the two flight conditions, particularly since the C_{D_0} values used to obtain C_{D_i} were obtained from generic F/A-18A wind-tunnel data. The trend is consistent at all longitudinal positions tested and since the peak reduction (approximately 50 percent) is similar for both flight conditions, the results indicate the vortex size and strength (and corresponding influence on drag reduction) vary with flight condition. Testing at additional flight conditions is recommended to explore this concept further. It would be advantageous to be able to model vortex effects on C_{D_i} at one flight condition and have that model apply to all other flight conditions, as the theory would imply.

From the data, the optimum location for a majority of the test points ranges between $-0.25\ b < Y < -0.05\ b$ laterally and $-0.125\ b < Z < 0\ b$ vertically. The most significant reduction in C_{D_i} occurred at condition 1 and $X = 4.4\ b$, where the induced drag reduction was calculated to be 52 percent $Y = -0.44\ b$ and $Z = -0.13\ b$. At $X = 3.0\ b$, a peak reduction in C_{D_i} of 49.7 percent was calculated.

In general, the trends generated for C_{D_i} agree with those calculated for total drag, except with increased magnitude for each longitudinal station and flight condition. The optimum position for both total drag and induced drag also agree, as expected. The trend in the magnitude of C_{D_i} reduction, to have an increased peak value at increased Mach number and altitude condition, is contrary to the results shown for total drag, where the opposite is true. However, this trend is explained through the relationship of C_{D_i} and C_D as discussed previously. It is understood that the AFF program merely captured a sample of the complete picture, with only two flight conditions investigated. A more exhaustive flight program would be better able to discern the effects of Mach number and altitude separately, as well as bound the ranges over which increases or decreases in these performance parameters are calculated.

Improvement in Fuel Efficiency

The fuel flow reduction data were obtained at the same test points and specific time slices as the drag reduction data presented previously. Fuel-flow data were more sensitive to the actual time slice used within the vortex, because value varied as the pilot or ATC continually modulated the throttle to maintain the prescribed nose-to-tail separation or flight conditions. After choosing an initial segment of data to best meet position and drag data quality requirements, the time slice within a test point was then adjusted (enlarged, reduced, or shifted) to improve the quality of the fuel-flow data. This adjustment was required

because of the cyclic nature of the fuel-flow data that occurs as the pilot or automatic-throttle attempts to maintain constant speed by modulating the throttle. When possible, complete cycles of throttle movement were used, as opposed to partial cycles that tended to bias the fuel-flow results high or low. In addition, changes in the lead airplane fuel-flow data during a test point were used to adjust the trailing airplane data to account for gust and turbulence effects encountered by both aircraft.[3]

One area of interest regarding fuel-flow reduction was the concern that excessive throttle use (high rates and amplitudes) could adversely affect the results. The AFF pilots were conscious of this concern and made every attempt to minimize throttle use while in formation when ATC was not engaged. In some cases however, atmospheric turbulence had a profound affect on the ability of the lead airplane autopilot to maintain constant speed and altitude. Consequently, this increased the workload of the trail pilot to keep the airplane in proper formation position and ultimately had an unfavorable affect on fuel flow. An example of this occurrence is presented in figure 9. Drag coefficient, fuel flow rate, and Mach number are all plotted for the same test point. A significant drag reduction was successfully demonstrated and the drag data was fairly consistent (fig. 9). Upon further analysis, additional qualities of the test point appear. While the trail airplane was on-conditions in the vortex, the two-airplane formation was upset by a wind gust. The Mach number of the lead airplane fluctuated, and the autopilot of the vehicle compensated to stay on-conditions. The manually-flown trail airplane was also upset by the same gust and the pilot had to correct for large and dynamic variations in the separation distance from the lead airplane. To overcome this, the pilot greatly increased the frequency and amplitude of throttle movement to maintain proper separation. The result was that the trailing airplane actually measured more fuel use in the vortex than during the baseline because of excessive throttle usage, even though significant drag reduction was realized. This illustrates the need for designers of autonomous-position control laws to minimize the gain on throttle use to maintain longitudinal separation, particularly since fuel (and drag) reduction shows little sensitivity to longitudinal position. The affects of longitudinal position on drag and fuel flow are discussed in detail in the next section.

Figures 10 and 11 show line plots of fuel flow as a function of lateral spacing (wing overlap) at various vertical offsets. While a relatively complete matrix of data was gathered at the $X = 3.0 \ b$, $4.4 \ b$, and $6.6 \ b$ stations, no fuel reduction data was obtained at the $X = 2.0 \ b$ location because slide-out maneuvers were not conducted. At this condition, automatic-throttle was considered unsafe and slide-outs to baseline conditions could not be performed. The concern was that the close proximity of the trail airplane to the lead airplane required positive control of the throttle at all times. An attempt was made to estimate the baseline fuel-flow values as a function of vehicle weight, just like the baseline drag values were obtained for this condition. Whereas the baseline drag data showed a strong correlation to vehicle gross weight (which affects trim angle-of-attack), the fuel flow data was inconsistent. Therefore, no fuel reduction data was obtained at the $X = 2.0 \ b$ condition.

At $X = 3.0 \ b$, the optimal position was shown to be between $-0.22 \ b < Y < -0.10 \ b$ lateral wing overlap and $-0.125 \ b < Z < 0.0 \ b$ vertical offset at both flight conditions. As plotted in figures 10(b) and 11(b), the maximum improvements in fuel flow were measured to be approximately 18.6 percent at condition 1 and 12.2 percent at condition 2.

At $X = 4.4 \ b$, as it was shown at $X = 3.0 \ b$, the optimal position was shown to be between $-0.20 \ b < Y < -0.10 \ b$ wing overlap and a vertical offset of $-0.125 \ b < Z < 0.0 \ b$ at condition 1. The largest improvement in fuel efficiency at this condition was measured to be approximately 18.5 percent (fig. 10(c)). At condition 2, the fuel flow reduction shown in figure 11(c) reduces slightly to 16.5 percent at $Z = 0.0 \ b$ and $Y = -0.20 \ b$.

22
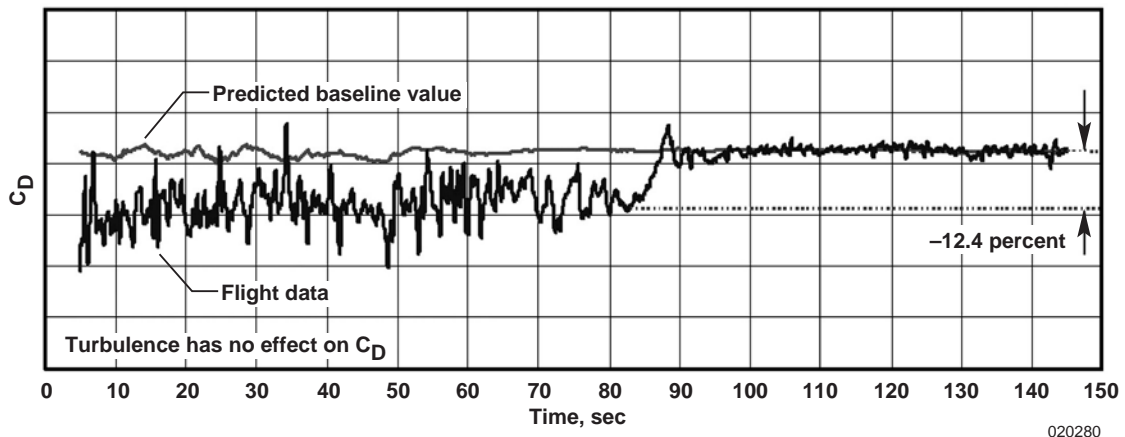
(a) No effect on C_D
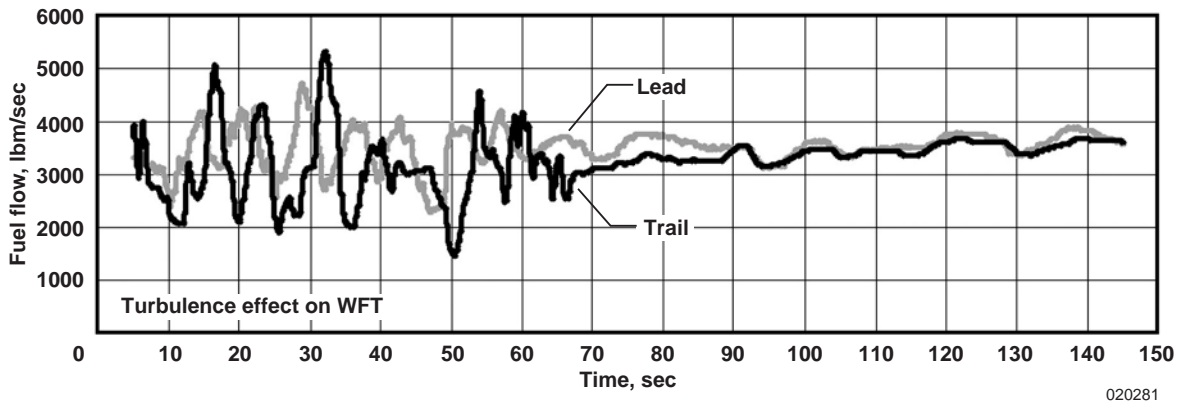
(b) Effect on WFT
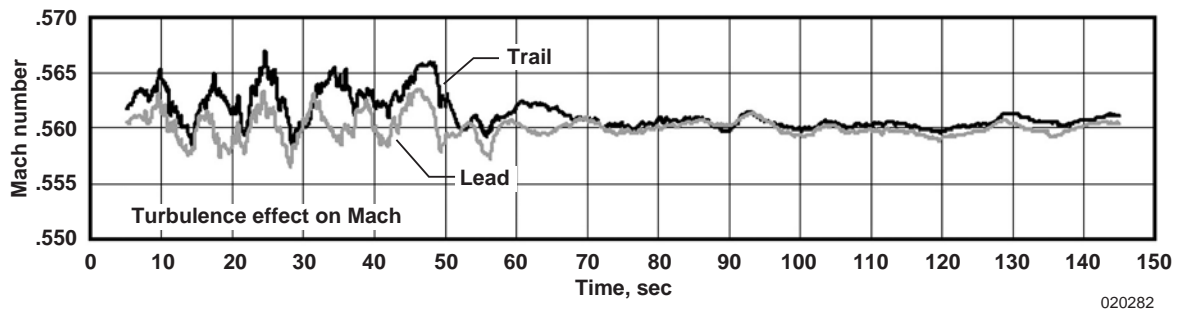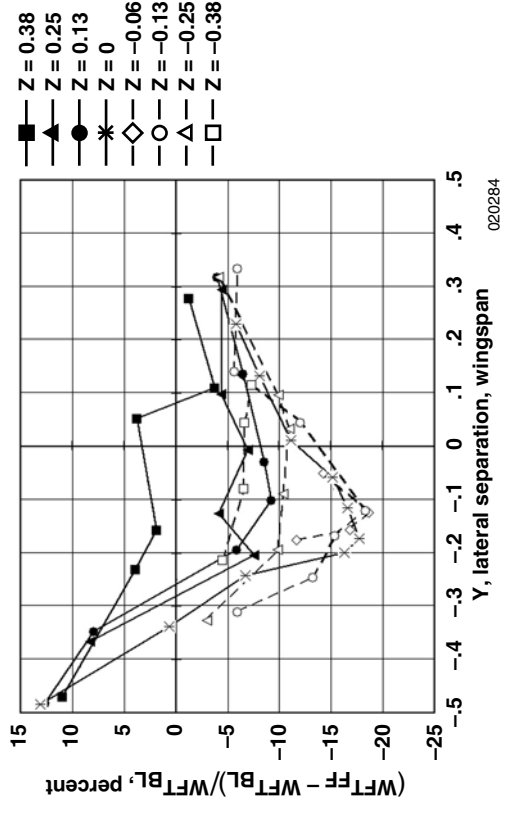

(c) Effect on Mach number

Figure 9. Example of drag reduction without associated fuel-flow reduction as a result of excessive throttle use.
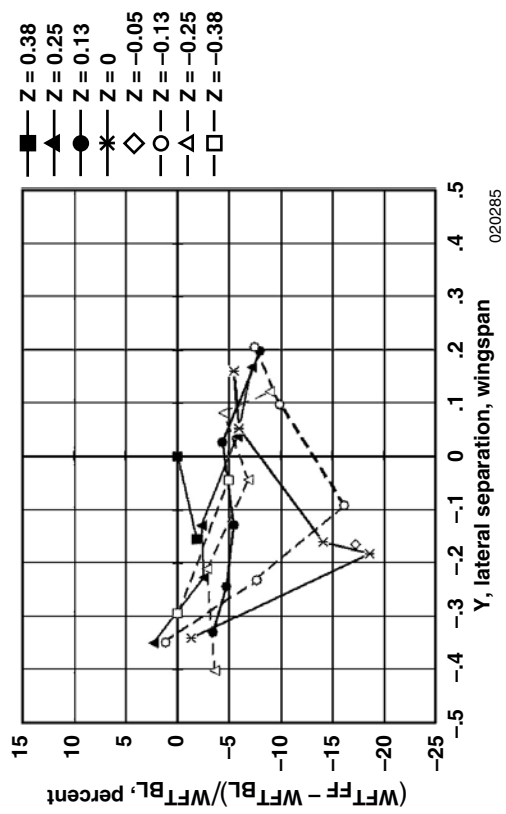
(b) X = 3.0 b

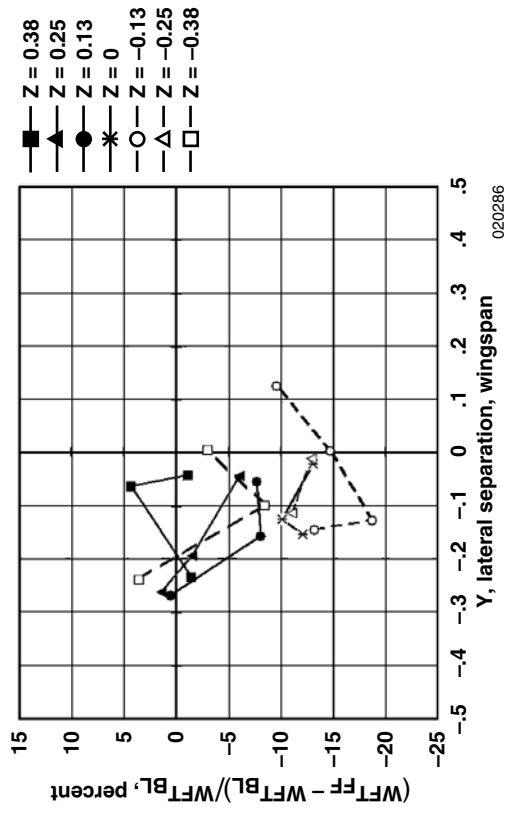Z = 0.38
Z = 0.25
Z = 0.13
Z = 0
Z = −0.06
Z = −0.13
Z = −0.25
Z = −0.38

020284

Y, lateral separation, wingspan

$(WFT_{FF} - WFT_{BL})/WFT_{BL}$, percent

(d) X = 6.6 b

Z = 0.38
Z = 0.25
Z = 0.13
Z = 0
Z = −0.13
Z = −0.25
Z = −0.38

020286

Y, lateral separation, wingspan

$(WFT_{FF} - WFT_{BL})/WFT_{BL}$, percent

No data
available

020283

(a) X = 2.0 b

(c) X = 4.4 b

Z = 0.38
Z = 0.25
Z = 0.13
Z = 0
Z = −0.05
Z = −0.13
Z = −0.25
Z = −0.38

020285

Y, lateral separation, wingspan

$(WFT_{FF} - WFT_{BL})/WFT_{BL}$, percent
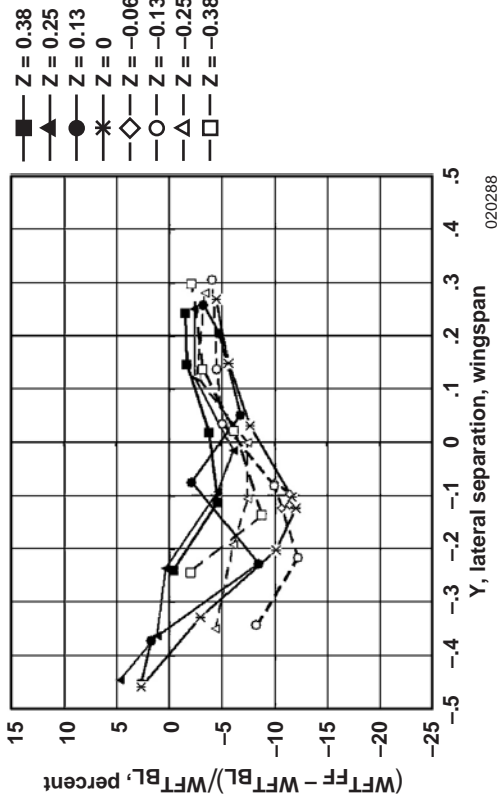
Figure 10. Demonstrated change in fuel-flow for the trailing airplane in formation flight at condition 1, four longitudinal separations.

No data
available

020283

(a) $X = 2.0\,b$

Z = 0.38
Z = 0.25
Z = 0.13
Z = 0
Z = −0.06
Z = −0.13
Z = −0.25
Z = −0.38

15
10
5
0
−5
−10
−15
−20
−25

$(WFT_{FF} - WFT_{BL})/WFT_{BL}$, percent

−.5 −.4 −.3 −.2 −.1 0 .1 .2 .3 .4 .5

Y, lateral separation, wingspan

020288

(b) $X = 3.0\,b$

Z = 0.38
Z = 0.25
Z = 0.13
Z = 0
Z = −0.13
Z = −0.25
Z = −0.38

15
10
5
0
−5
−10
−15
−20
−25

$(WFT_{FF} - WFT_{BL})/WFT_{BL}$, percent

−.5 −.4 −.3 −.2 −.1 0 .1 .2 .3 .4 .5

Y, lateral separation, wingspan

020289

(c) $X = 4.4\,b$

Z = 0.38
Z = 0.25
Z = 0.13
Z = 0
Z = −0.13
Z = −0.25
Z = −0.38

15
10
5
0
−5
−10
−15
−20
−25

$(WFT_{FF} - WFT_{BL})/WFT_{BL}$, percent

−.5 −.4 −.3 −.2 −.1 0 .1 .2 .3 .4 .5

Y, lateral separation, wingspan

020290

(d) $X = 6.6\,b$

Figure 11. Demonstrated change in fuel-flow for the trailing airplane in formation flight at condition 2, four longitudinal separations.
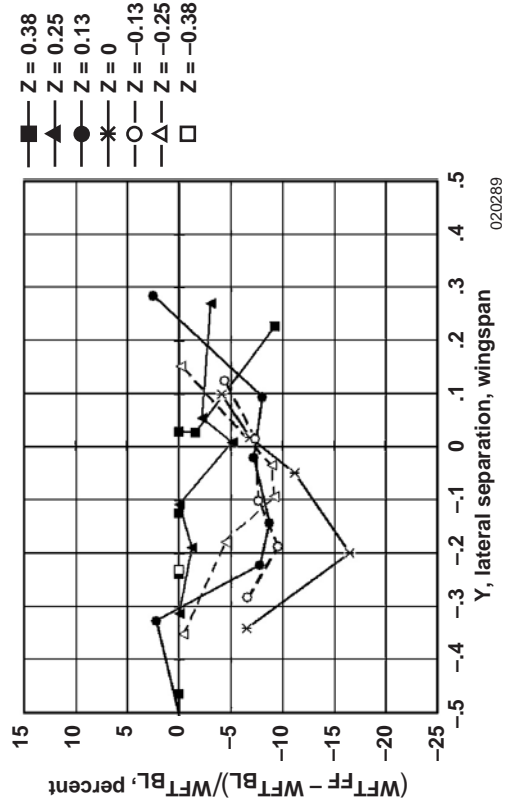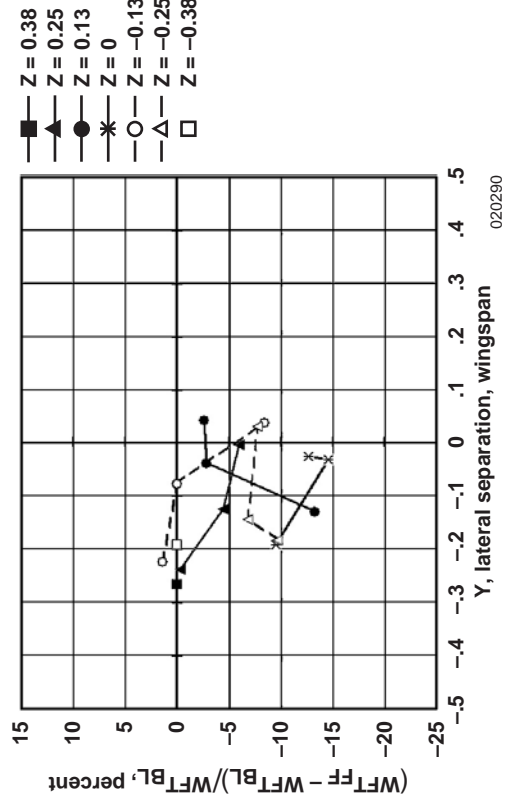
For $X = 6.6$ b, compare figures 10(d) and 11(d). At condition 1, a maximum fuel flow reduction of 18.7 percent was shown to be at $Y = -0.125$ b and $Z = -0.125$ b vertical offset. At condition 2, as was shown in the drag data, the region of optimal fuel flow reduction moves outboard to a location between -0.15 $b < Y < 0.0$ b laterally and -0.05 $b < Z < 0.05$ b vertically. At this location, the greatest improvement in fuel flow was shown to be -14.6 percent.

Figure 12 shows the same data set as figures 10 and 11, presented as a contour plot, as discussed previously. This figure provides a better depiction of the size and magnitude of the region of benefit at each flight condition based on vertical and lateral position. These plots closely resemble the shape of those developed previously for total drag and induced drag. The greatest fuel-flow reductions occurred at the slower and lower flight condition, condition 1. At this condition, the fuel flow data at $X = 3.0$ b, 4.4 b, and 6.6 b separations show a similar region of maximum benefit, located at the approximate center of the matrix of data, a lateral offset of -0.20 $b < Y < -0.10$ b wing overlap and a vertical station of -0.15 $b < Z < -0.05$ b.

There are several data points in figures 5, 6, 10, and 11 that do not appear to follow the prevailing trend of the data set. A gradual improvement in fuel efficiency is expected as the *optimal* vertical and lateral position is approached. Instead, these peculiar points appear to spike to an almost 15-percent degradation in fuel efficiency near the perceived optimal position. Because this peculiarity has been demonstrated at several vertical offsets and two different flight conditions, the phenomenon cannot be attributed to data scatter. Aside from attributing it to vortex randomness or uncertainty in the data, a possible explanation for this is the dynamic use of throttle to maintain station during these test points. Influenced by many factors, it is easy to see that the throttle setting (and hence fuel flow rate) could be biased high or low for a particular time slice, inconsistent with data at nearby test points.

Overall, the fuel-flow reduction data trends are similar in shape and magnitude to the C_D data, averaging 2-3 percent less in overall magnitude at condition 1 but with varied results (sometimes a greater percentage of reduction) at condition 2. These results give confidence to the overall drag reduction values. The peak location is fairly constant at condition 1 for all longitudinal stations, but appears to move around somewhat as a function of longitudinal station at condition 2. All three longitudinal positions show approximately the same peak magnitude in fuel flow reduction at condition 1 and show mixed results at condition 2.

As the trailing airplane moves closer, simple theory predicts the lead airplane will benefit slightly (up to 3 percent) from interacting with the flow field of the trailing airplane while in formation.[10] Although fuel flow was specifically monitored on the lead airplane during formations as close as $X = 2.0$ b, overall it was found the trailing airplane had no noticeable effect on the fuel-flow values of the lead airplane.

## Effects of Longitudinal Separation on Performance Benefits

Dedicated test points were flown in this program to address the changes in drag and fuel flow as a function of increasing longitudinal spacing. At condition 1, the optimum lateral and vertical positions ($Y = -0.19$ b, $Z = -0.06$ b) were flown at sequential trailing positions to obtain this data. This optimum position was selected based upon limited processed flight data available at the time, and although the optimum position has been shown to vary somewhat at each longitudinal station, it is important to mention that this single position was maintained for these particular test points. Additional data from the matrix of test points flown previously were also used to augment the analysis. Figure 13 shows the results from this focused study. The trends for airplane total drag coefficient, induced drag coefficient, and fuel
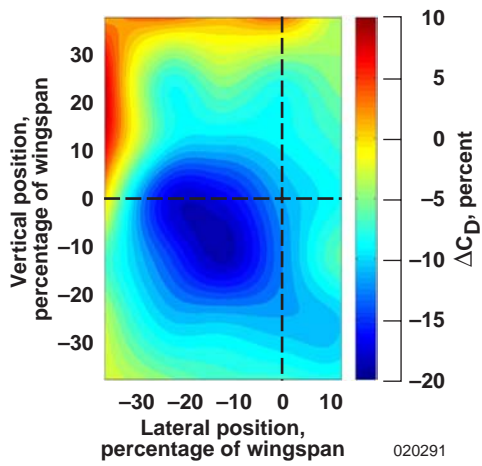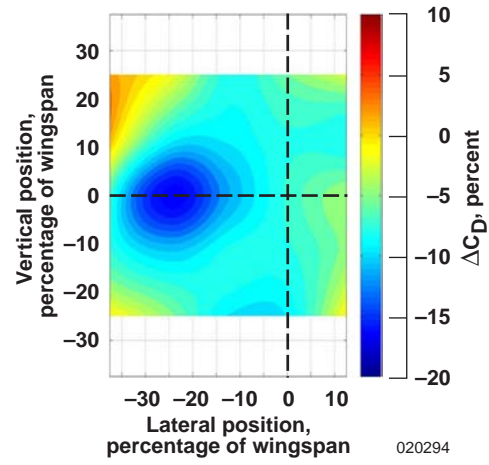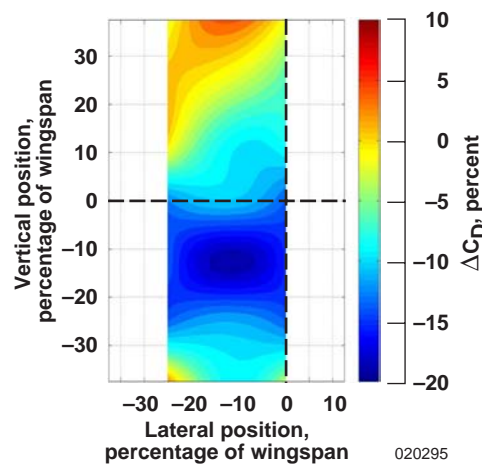
(a) $X = 3.0\ b$, condition 1
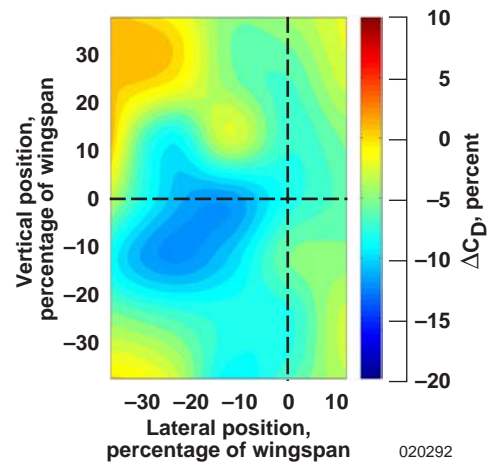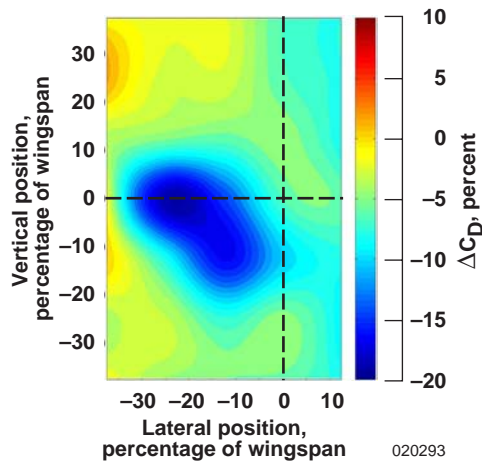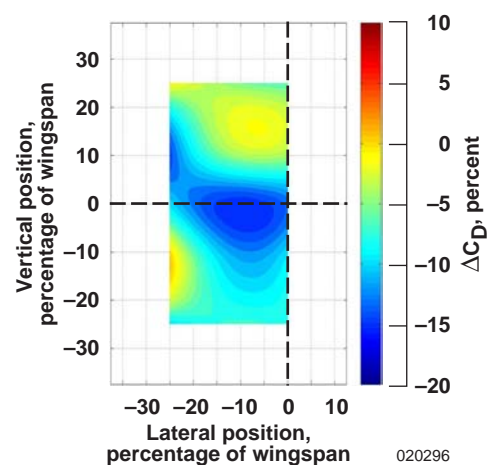
(b) $X = 3.0\ b$, condition 2

(c) $X = 4.4\ b$, condition 1

(d) $X = 4.4\ b$, condition 2

(e) $X = 6.6\ b$, condition 1

(f) $X = 6.6\ b$, condition 2

Figure 12. Summary of fuel flow (WFT) reduction contour plots as a function of Y-Z position at conditions 1 and 2.

efficiency are similar for each of the three parameters, and show the best benefits were found at a separation of 100 ft nose-to-tail ($X = 4.2$ b). This is close to the prediction shown by Blake and Multhopp,[7] which uses the horseshoe vortex model for predicting the vortex effects. This is discussed in more detail in Ray (ref. 3). Further aft, the benefits begin to slowly diminish as a result of viscous effects, but are still significant.

Each data set has been banded with estimated maximum and minimum curves, based on available data, to provide an estimated range of potential values for each parameter. This is an attempt to compensate for any potential scatter in the data, while capturing a smooth trend for each parameter. As can be seen in figure 13, the scatter grows larger with increasing longitudinal separation—a function of decreased data availability and increased uncertainty in vortex location and maximum strength.

Figure 13 shows good agreement between the drag coefficients and fuel flow. Each band of data appears to follow the same trend. When the drag on the airplane is reduced, the engine power demand is decreased and fuel flow demand is decreased as expected.
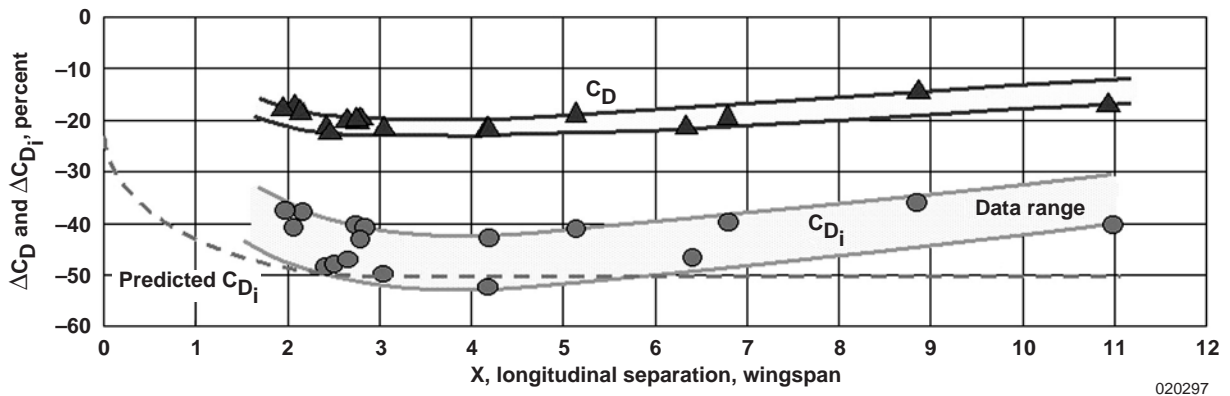
(a) Drag
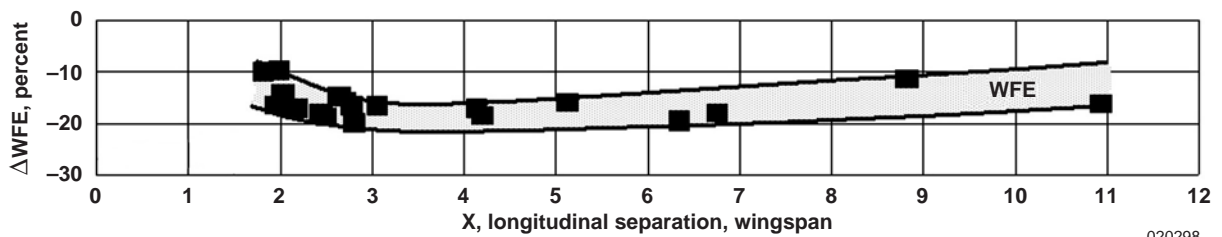
(b) Fuel flow

Figure 13. Drag and fuel flow change as a function of longitudinal separation at condition 1, $Y = -0.18$ to 0.18 and $Z = -0.10$ to 0.0.

28

The predicted C_{D_i} line represents theoretical analysis. The simple theory presented by Hoerner[9] shows that the total induced drag for a system of aircraft remains constant. This trend shows a reduction in C_{D_i} benefit as the trail airplane longitudinal separation gets smaller than $X = 3.0\ b$. This may be because theoretically the benefits begin to be transferred to the lead airplane. As mentioned previously, no improvements in fuel flow were demonstrated for the lead airplane at any of the conditions tested during this program and drag was not calculated for this airplane.

Pilot comments indicate that the vortex position was not as stable further aft and seemed to wander around somewhat. The scatter in the data seems to confirm this. Nonetheless, the results show a large tolerance in longitudinal position while still showing large performance benefits. This is of even more significance from the standpoint of designing an autonomous controller to exploit these demonstrated performance benefits. To maintain longitudinal spacing with the engine, a low-gain controller can be used, minimizing fuel usage. Had this not been demonstrated, more rapid throttle movements might have to be used to hold a more precise position, using excessive amounts of fuel and negating the performance benefit of formation flight. More information on how the vortex moves around at the further aft locations would benefit control law development. Based on the data gathered during the AFF program, the optimum location can be expected to move around at longitudinal locations further than 5 wingspans aft ($X > 5.0$). The results also indicate a control law design that is able to continuously seek the optimum position probably makes the most sense because of vortex movement, particularly at positions aft of the optimum longitudinal location.

CONCLUSIONS

With two highly-instrumented F/A-18 airplanes, the Autonomous Formation Flight program at NASA Dryden Flight Research Center (Edwards Air Force Base, California) was able to demonstrate a number of significant results proving the value of continued development of autonomous systems for formation flight. Controllable flight under the influence of the wingtip vortex of a lead airplane is possible, and can even be accomplished without autonomous systems, by providing positioning cues to the pilot on a heads-up display. Conveniently, the area of the vortex that yields the most beneficial C_D is located within the region of controllable flight. This region is also large enough at two flight conditions to make its exploitation quite feasible. The changes in lift and drag coefficient were evaluated for each maneuver by comparing drag while in the vortex with baseline values. In general, very small changes in the calculated average lift coefficient were found for all conditions, affirming that the change in drag coefficient is attributed to a change in the induced drag component.

Maximum drag reductions of over 20 percent were calculated at condition 1 for longitudinal separations of X = 3.0 b and 4.4 b, and maximum reductions in total fuel flow were demonstrated up to 18 percent. Other longitudinal stations (X = 2.0 b and 6.6 b) showed similar results. Although simple theory predicts the trailing airplane can influence performance parameters for the lead airplane at close separation, no improvements in drag or fuel flow were demonstrated for the lead airplane at any of the conditions tested during this program.

The optimum drag reduction region was found to be at a vertical position range of $-0.10\ b < Z < 0.0\ b$ and a lateral position range of $-0.20\ b < Y < -0.10\ b$. All data show more sensitivity (steeper gradients) as the trailing airplane moves inboard of the leading airplane, compared to the outboard positions. In fact, drag *increases* were calculated at some high wing overlap positions, verifying the importance of proper station-keeping to obtain the best results. Even with noted changes in the shape and intensity of the

vortex at different flight conditions, optimal drag benefits (greater than 10 percent drag reduction) are apparent on all plots within a vertical position of -0.10 $b < Z < 0.0$ b and a lateral position of -0.25 $b < Y < -0.10$ b. Only one longitudinal station, $X = 6.6$ b, at condition 2 showed peak drag and fuel flow reductions in a different region, -0.15 $b < Y < -0.05$ b and -0.05 $b < Z < 0.05$ b.

Induced drag results compare favorably with a simple prediction model. The induced drag showed marked improvement up to 50 percent at all flight conditions and longitudinal stations. A comparison of the induced drag change for the two flight conditions revealed differences in the size of the *Y-Z* region of benefit, indicating the vortex size may vary as a function of flight condition.

The flight tests revealed a large tolerance in longitudinal position while still showing impressive performance benefits. The favorable effects of the vortex degrade gradually, with increased separation distances after peaking at an aft station equal to 100 ft nose-to-tail ($X = 4.2$ b). In designing an autonomous controller to exploit these demonstrated performance benefits, a low-gain controller for longitudinal position can be used, helping to reduce throttle movements and minimize fuel usage.

REFERENCES

1. Hanson, Curtis E., Jack Ryan, Michael J. Allen, and Steven R. Jacobson, "An Overview of Flight Test Results for a Formation Flight Autopilot," AIAA-2002-4755, AIAA GNC Conference, Aug. 5–8, 2002, Monterey, California.

2. Hansen, Jennifer L and Brent R. Cobleigh, "Induced Moment Effects of Formation Flight Using Two F/A-18 Aircraft," AIAA-2002-4489, AIAA Atmospheric Flight Mechanics Conference, August 5–8, 2002, Monterey, California.

3. Ray, Ronald J., Brent R. Cobleigh, M. Jake Vachon, and Clint St. John, "Flight Test Techniques Used to Evaluate Performance Benefits During Formation Flight," AIAA 2002-4492, Atmospheric Flight Mechanics Conference, August 5–8, 2002, Monterey, California.

4. Orme, John S., *Digital Performance Simulation Models of the F-15, F-16XL, F-18, F-104, TACT F-111, X-29 and Hypersonic Research Vehicle*, NASA/TM-104244, January 1992.

5. Ray, Ronald J., *Evaluation of Various Thrust Calculation Techniques on an F404 Engine*, NASA TP-3001, April 1990.

6. Wagner, Capt. Geno, LtCol Dave Jacques, Bill Blake, and Meir Pacher, "An Analytical Study Of Drag Reduction In Tight Formation Flight," AIAA 2001-4075, AIAA Atmospheric Flight Mechanics Conference, Montreal, Canada, August 6–9, 2001.

7. Blake, W., and Dieter Multhopp, "Design, Performance and Modeling Considerations for Close Formation Flight," AIAA-98-4343, AIAA Atmospheric Flight Mechanics Conference, Boston, Massachusetts, August 10–12, 1998.

8. Hummel, D., "The Use of Aircraft Wakes to Achieve Power Reductions in Formation Flight," AGARD-CP-584, *The Characterization and Modification of Wakes from Lifting Vehicles in Fluids*, Trondheim, Norway, May 1996.

9. Horner, Dr. Sighard F., *Fluid-Dynamic Drag*: *Practical Information on Aerodynamic Drag and Hydrodynamic Resistance.* Published by the Author, 1965.

10. Maskew, Brian, *Formation Flight Benefits Based on Vortex Lattice Calculations*, NASA/CR-151974, April 1977.

11. Anderson, John D., Jr., *Fundamentals of Aerodynamics*, McGraw-Hill, 1991, 1984.

REPORT DOCUMENTATION PAGE

Form Approved
OMB No. 0704-0188

1. AGENCY USE ONLY (Leave blank)	2. REPORT DATE September 2003	3. REPORT TYPE AND DATES COVERED Technical Memorandum	

4. TITLE AND SUBTITLE

F/A-18 Performance Benefits Measured During the Autonomous Formation Flight Project

6. AUTHOR(S)

M. Jake Vachon, Ronald J. Ray, Kevin R. Walsh, and Kimberly Ennix

5. FUNDING NUMBERS

706 35 00 E8 28 00 AFF

7. PERFORMING ORGANIZATION NAME(S) AND ADDRESS(ES)

NASA Dryden Flight Research Center
P.O. Box 273
Edwards, California 93523-0273

8. PERFORMING ORGANIZATION REPORT NUMBER

H-2505

9. SPONSORING/MONITORING AGENCY NAME(S) AND ADDRESS(ES)

National Aeronautics and Space Administration
Washington, DC 20546-0001

10. SPONSORING/MONITORING AGENCY REPORT NUMBER

NASA/TM-2003-210734

11. SUPPLEMENTARY NOTES

Presented at the AIAA Atmospheric Flight Mechanics Conference, Monterey, California, August 5–8, 2002.

12a. DISTRIBUTION/AVAILABILITY STATEMENT

Unclassified—Unlimited
Subject Category 05

This report is available at http://www.dfrc.nasa.gov/DTRS/

12b. DISTRIBUTION CODE

13. ABSTRACT (Maximum 200 words)

The Autonomous Formation Flight (AFF) project at the NASA Dryden Flight Research Center (Edwards, California) investigated performance benefits resulting from formation flight, such as reduced aerodynamic drag and fuel consumption. To obtain data on performance benefits, a trailing F/A-18 airplane flew within the wingtip-shed vortex of a leading F/A-18 airplane. The pilot of the trail airplane used advanced station-keeping technology to aid in positioning the trail airplane at precise locations behind the lead airplane. The specially instrumented trail airplane was able to obtain accurate fuel flow measurements and to calculate engine thrust and vehicle drag. A maneuver technique developed for this test provided a direct comparison of performance values while flying in and out of the vortex. Based on performance within the vortex as a function of changes in vertical, lateral, and longitudinal positioning, these tests explored design-drivers for autonomous station-keeping control systems. Observations showed significant performance improvements over a large range of trail positions tested. Calculations revealed maximum drag reductions of over 20 percent, and demonstrated maximum reductions in fuel flow of just over 18 percent.

14. SUBJECT TERMS

Drag reduction, Flight test techniques, Formation flight, Fuel reduction, Performance

15. NUMBER OF PAGES

36

16. PRICE CODE

17. SECURITY CLASSIFICATION OF REPORT Unclassified	18. SECURITY CLASSIFICATION OF THIS PAGE Unclassified	19. SECURITY CLASSIFICATION OF ABSTRACT Unclassified	20. LIMITATION OF ABSTRACT Unlimited